Electronic Supplementary Material (ESI) for Inorganic Chemistry Frontiers.
This journal is © the Partner Organisations 2024

Electronic Supporting Information (ESI)

Synthesis and Near-Infrared Photothermal Conversion of Cp*Rh-Based [2]-Catenanes in Trapezoidal Metallacycle

Pan-Pan Hua,[a] Hui-Jun Feng,[a,b]* Xiang Gao,[b] Li-Fang Zhang[a] and Guo-Xin Jin[b]*

[a] *Key Laboratory of Magnetic Molecules and Magnetic Information Materials of the Ministry of Education, School of Chemistry and Material Science, Shanxi Normal University, Taiyuan 030031, China*

[b] *Shanghai Key Laboratory of Molecular Catalysis and Innovative Materials; State Key Laboratory of Molecular Engineering of Polymers, Department of Chemistry, Fudan University, Shanghai 200433, P. R. China.*

*E-mail: gxjin@fudan.edu.cn.

Table of Contents

1. Experimental Procedures

Synthetic Procedures:

Synthesis of L1.

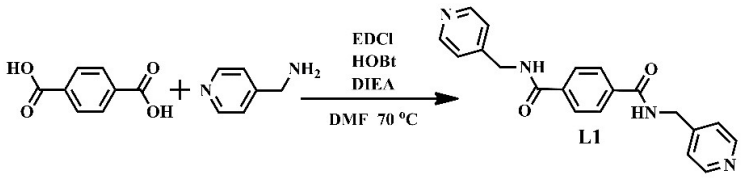

Scheme 1. Synthesis of **L1**.

Terephthalic acid (132.9 mg, 0.8 mmol), 4-Pyridinemethaneamine (162.4 μL, 1.6 mmol), HOBt (0.10 g, 0.8 mmol), EDCI (0.13 g, 0.8 mmol), and DIEA (0.4 mL, 2.0 mmol) were mixed in DMF (10 mL) and the mixture was stirred at 70 °C. After 2 d, the solution was concentrated by evaporation. Adding a saturated solution of sodium bicarbonate to the above reactants yields a solid, which was then filtered to obtain **L1** (238.3 mg; Yield: 86%). Anal. calcd for $C_{20}H_{18}N_4O_2$: C, 69.35; H, 5.24; N, 16.17. Found: C, 69.45; H, 5.36; N, 16.24. ^{1}H NMR (600 MHz, DMSO, ppm) δ = 9.28 (s, 2H), 8.52 (s, 4H), 8.03 (s, 4H), 7.33 (s, 4H), 4.54 (s, 4H). ^{13}C NMR (151 MHz, DMSO) δ 166.36 (s), 150.04 (s), 148.88 (s), 136.94 (s), 127.87 (s), 122.64 (s), 42.31 (s).

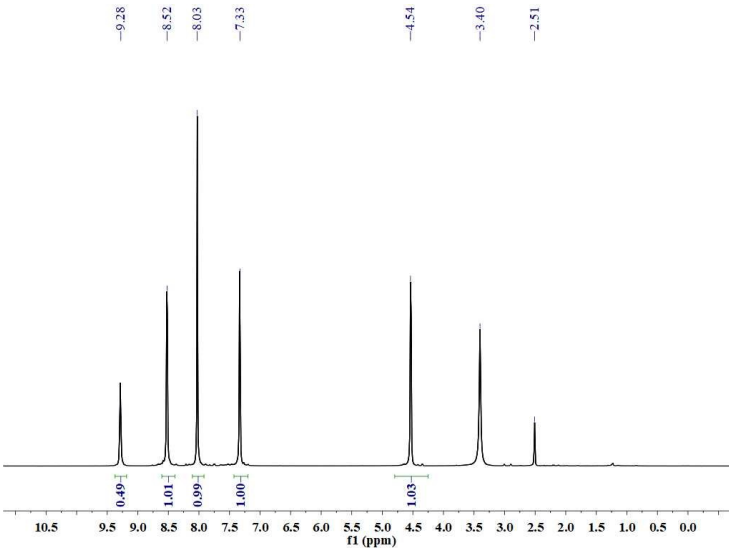

Fig. S1 ^{1}H NMR (600 MHz, DMSO-*d*6, ppm) for **L1**.

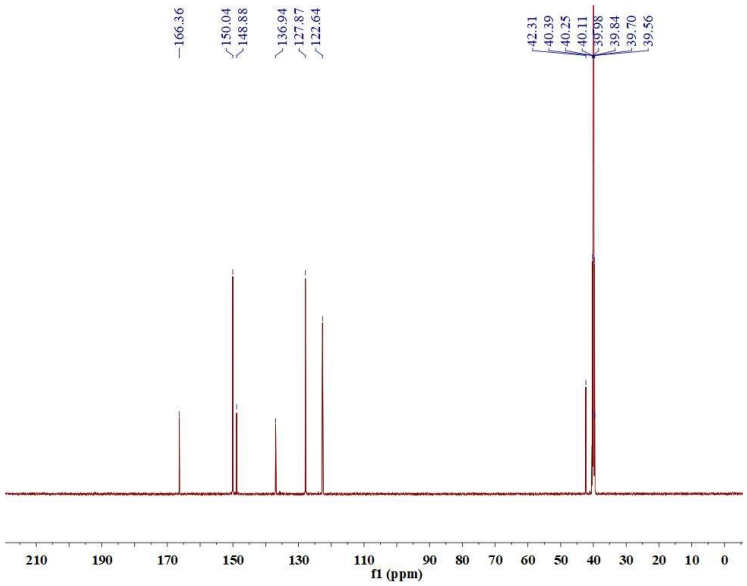

Fig. S2 ^{13}C NMR (151 MHz, DMSO-*d*6, ppm) for **L1**.

Synthesis of L2.

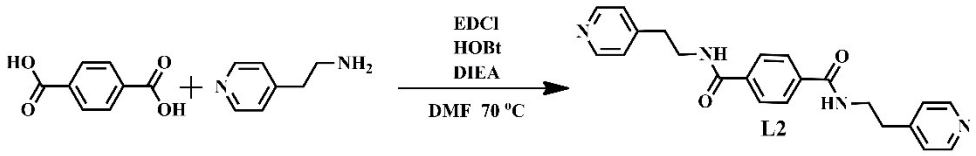

Scheme 2. Synthesis of **L2**.

Terephthalic acid (132.9 mg, 0.8 mmol), 4-(2-Aminoethyl)pyridine (191.0 μL, 1.6 mmol), HOBt (0.10 g, 0.8 mmol), EDCI (0.13 g, 0.8 mmol), and DIEA (0.4 mL, 2.0 mmol) were mixed in DMF (10 mL) and the mixture was stirred at 70 °C. After 2 d, the solution was concentrated by evaporation. By adding a saturated solution of sodium bicarbonate to the reactants mentioned above, a solid is formed. This solid was subsequently filtered to obtain **L2** (245.5 mg; Yield: 82%). Anal. calcd for $C_{22}H_{22}N_4O_2$: C, 70.57; H, 5.92; N, 14.96. Found: C, 70.42; H, 5.86; N, 14.82. ^{1}H NMR (600 MHz, DMSO, ppm) δ = 8.70 (s, 2H), 8.47 (s, 4H), 7.87 (s, 4H), 7.27 (s, 4H), 3.55 (s, 4H),

2.89 (s, 4H). ^{13}C NMR (151 MHz, DMSO) δ = 166.11 (s), 149.92 (s), 148.88 (s), 137.13 (s), 127.57 (s), 124.73 (s), 40.51 (s), 34.60 (s).

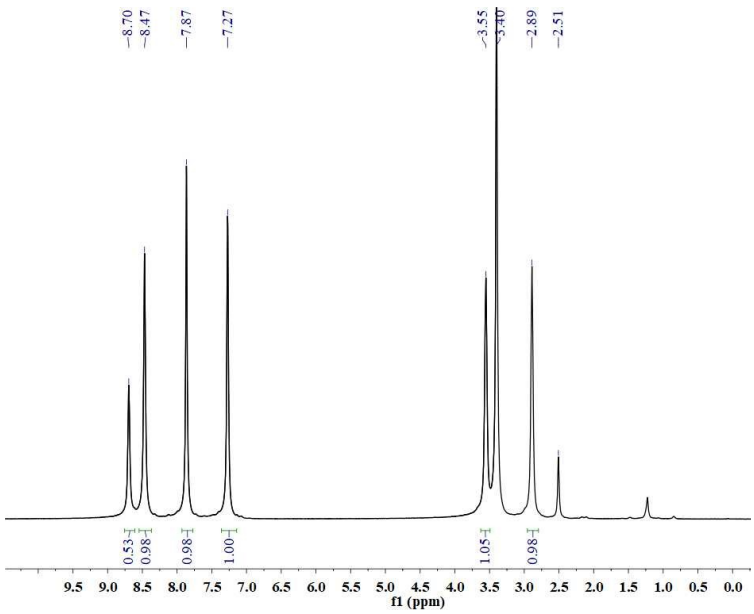

Fig. S3 ^{1}H NMR (600 MHz, DMSO-*d*6, ppm) for **L2**.

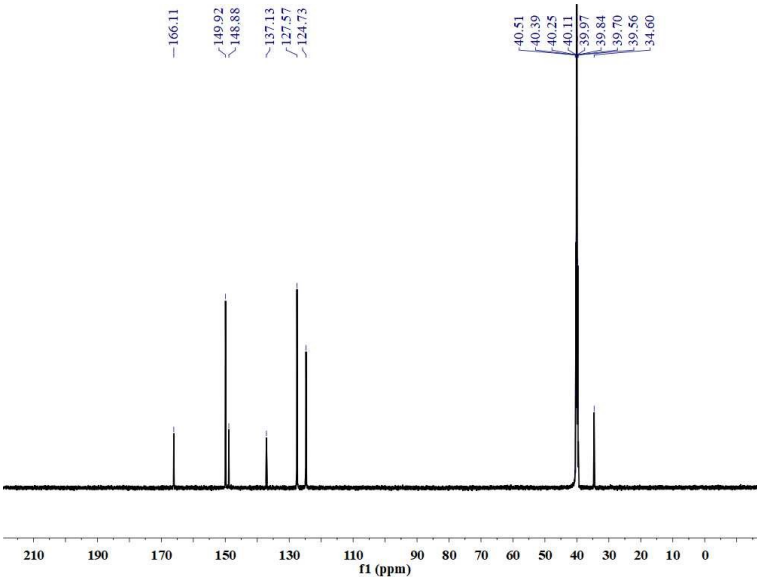

Fig. S4 ^{13}C NMR (151 MHz, DMSO-*d*6, ppm) for **L2**.

Synthesis of L3.

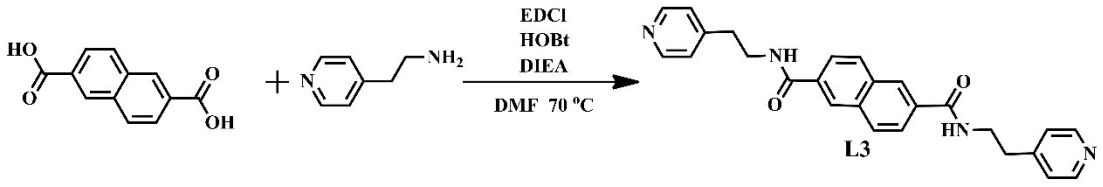

Scheme 3. Synthesis of **L3**.

Biphenyl-4,4'-dicarboxylic acid (193.8 mg, 0.8 mmol), 4-(2-Aminoethyl)pyridine (191.0 μL, 1.6 mmol), HOBt (0.10 g, 0.8 mmol), EDCI (0.13 g, 0.8 mmol), and DIEA (0.4 mL, 2.0 mmol) were mixed in DMF (10 mL) and the mixture was stirred at 70 °C. After 2 d, the solution was concentrated by evaporation. By adding a saturated solution of sodium bicarbonate to the reactants mentioned above, a solid is formed. This solid was subsequently filtered to obtain **L3** (295.4 mg; Yield: 87%). Anal. calcd for $C_{26}H_{24}N_4O_2$: C, 73.56; H, 5.70; N, 13.20. Found: C, 73.48; H, 5.81; N, 13.42. ^{1}H NMR (600 MHz, DMSO, ppm) δ = 8.81 (s, 2H), 8.48 (d, J = 3.6 Hz, 4H), 8.43 (s, 2H), 8.08 (d, J = 8.4 Hz, 2H), 7.95 (d, J = 8.4 Hz, 2H), 7.31 (d, J = 4.2 Hz, 4H), 3.61 (d, J = 5.9 Hz, 4H), 2.93 (t, J = 6.8 Hz, 4H). ^{13}C NMR (151 MHz, DMSO) δ 166.59 (s), 149.96 (s), 148.91 (s), 133.73 (s), 129.43 (s), 127.54 (s), 125.30 (s), 124.75 (s), 40.42 (s), 34.68 (s).

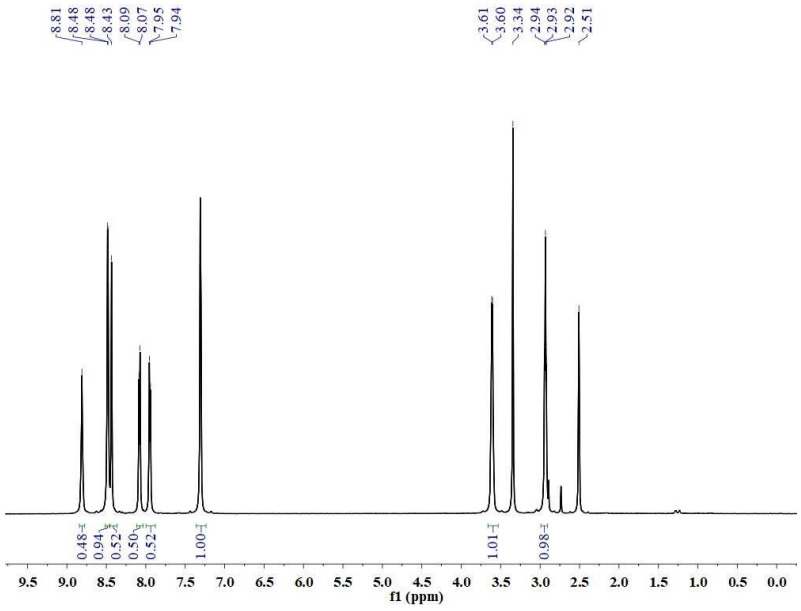

Fig. S5 ^{1}H NMR (600 MHz, DMSO-*d*6, ppm) for **L3**.

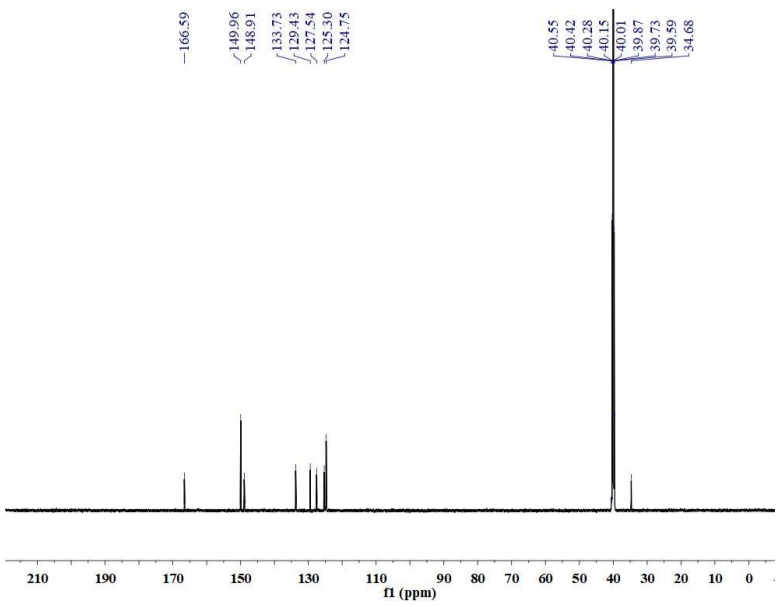

Fig. S6 ^{13}C NMR (151 MHz, DMSO-*d*6, ppm) for **L3**.

Synthesis of L4.

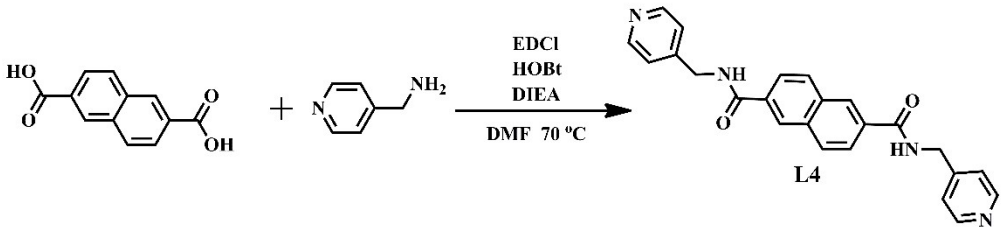

Scheme 4. Synthesis of **L4**.

Biphenyl-4,4'-dicarboxylic acid (193.8 mg, 0.8 mmol), 4-Pyridinemethaneamine (162.4 μL, 1.6 mmol), HOBt (0.10 g, 0.8 mmol), EDCI (0.13 g, 0.8 mmol), and DIEA (0.4 mL, 2.0 mmol) were mixed in DMF (10 mL) and the mixture was stirred at 70 °C. After 2 d, the solution was concentrated by evaporation. By adding a saturated solution of sodium bicarbonate to the reactants mentioned above, a solid is formed. This solid was subsequently filtered to obtain **L4** (269.6 mg; Yield: 85%). Anal. calcd for $C_{24}H_{20}N_4O_2$: C, 72.71; H, 5.08; N, 14.13. Found: C, 72.81; H, 5.15; N, 14.37. ^1H NMR (600 MHz, DMSO, ppm) δ = 9.38 (t, J = 5.9 Hz, 2H), 8.59 (s, 4H), 8.53 (d, J = 5.7 Hz, 2H), 8.16 (d, J = 8.5 Hz, 2H), 8.06 (d, J = 9.6 Hz, 2H), 7.37 (d, J = 5.7 Hz, 4H), 4.58

(d, J = 5.9 Hz, 4H). ^{13}C NMR (151 MHz, DMSO) δ 166.89 (s), 150.05 (s), 148.97 (s), 133.91 (s), 133.43 (s), 129.62 (s), 127.88 (s), 125.42 (s), 122.67 (s), 42.38 (s).

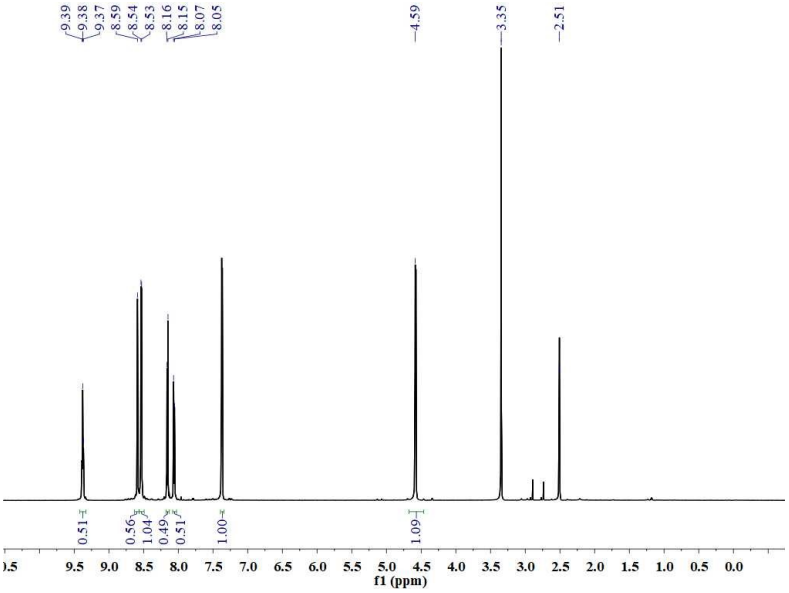

Fig. S7 ^{1}H NMR (600 MHz, DMSO-*d*6, ppm) for **L4**.

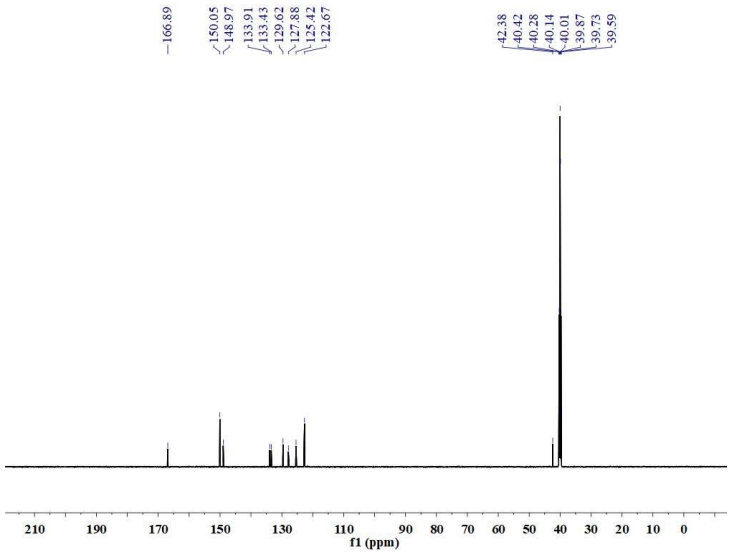

Fig. S8 ^{13}C NMR (151 MHz, DMSO-*d*6, ppm) for **L4**.

2. NMR Data

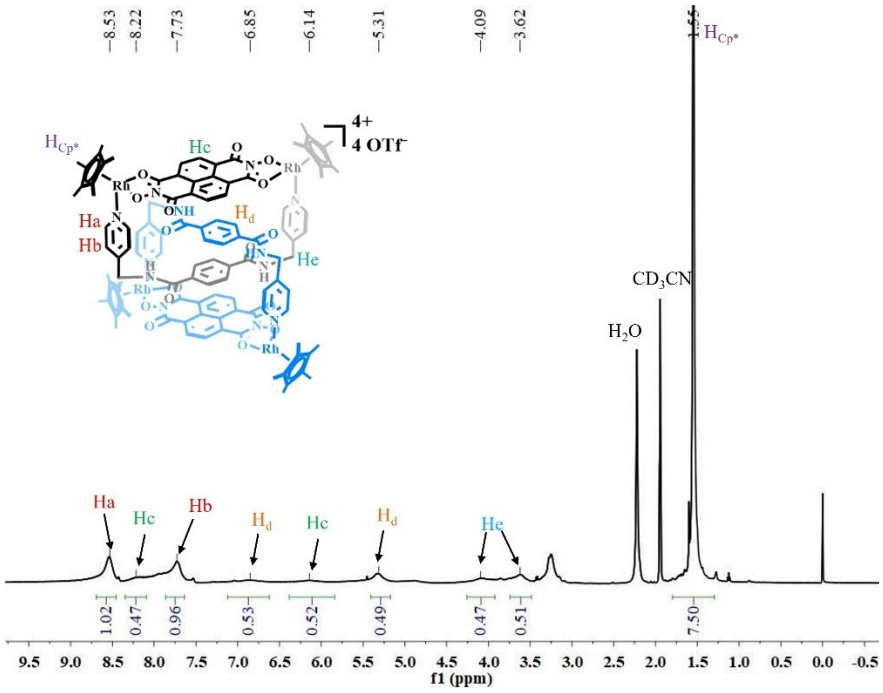

Fig. S9 ^{1}H NMR at 300K (600 MHz, CD_3CN, ppm) for **1**.

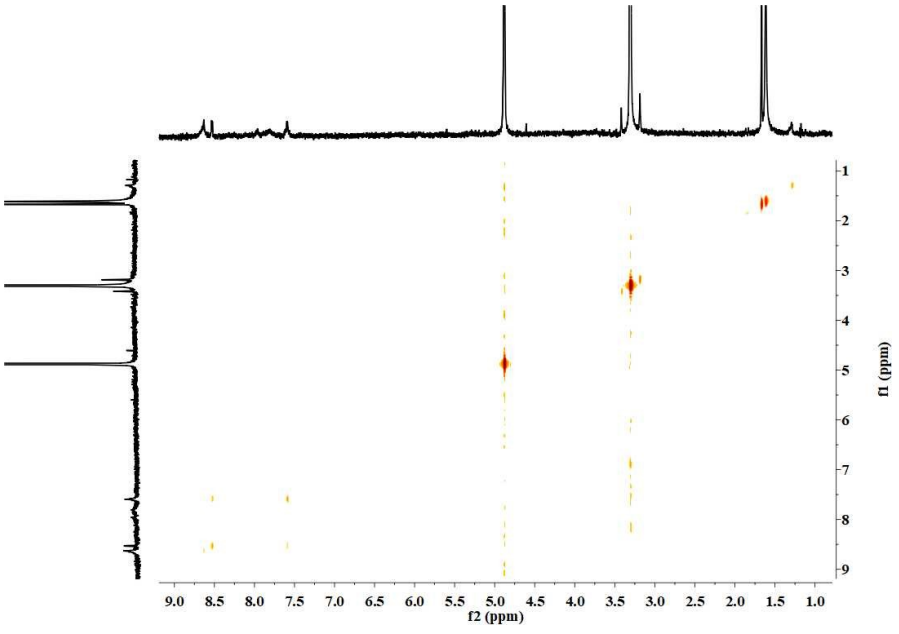

Fig. S10 ^{1}H - ^{1}H COSY NMR spectrum of **1** (600 MHz, CD_3CN) at 300K.

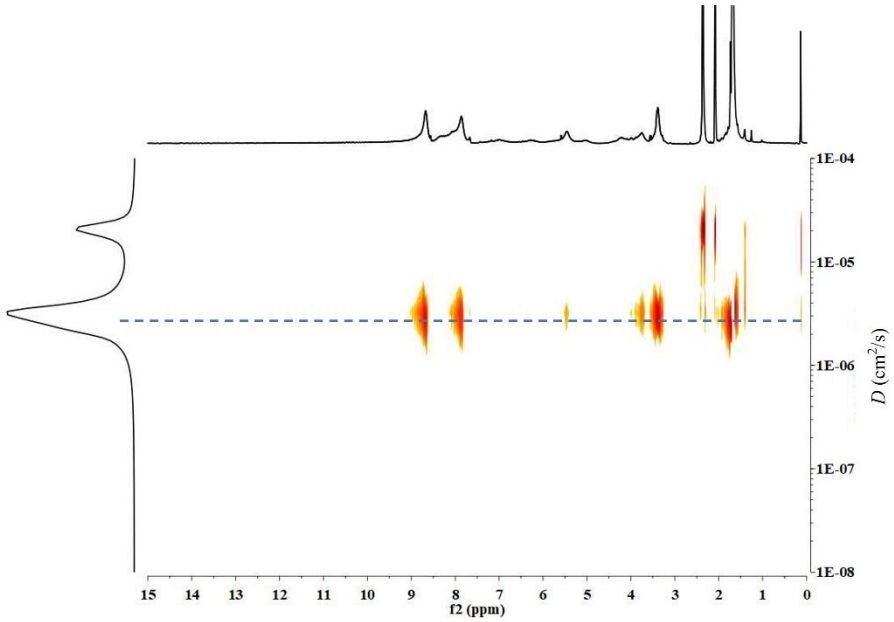

Fig. S11: ^{1}H DOSY NMR spectrum of **1** (600 MHz, CD_3CN) at 300K.

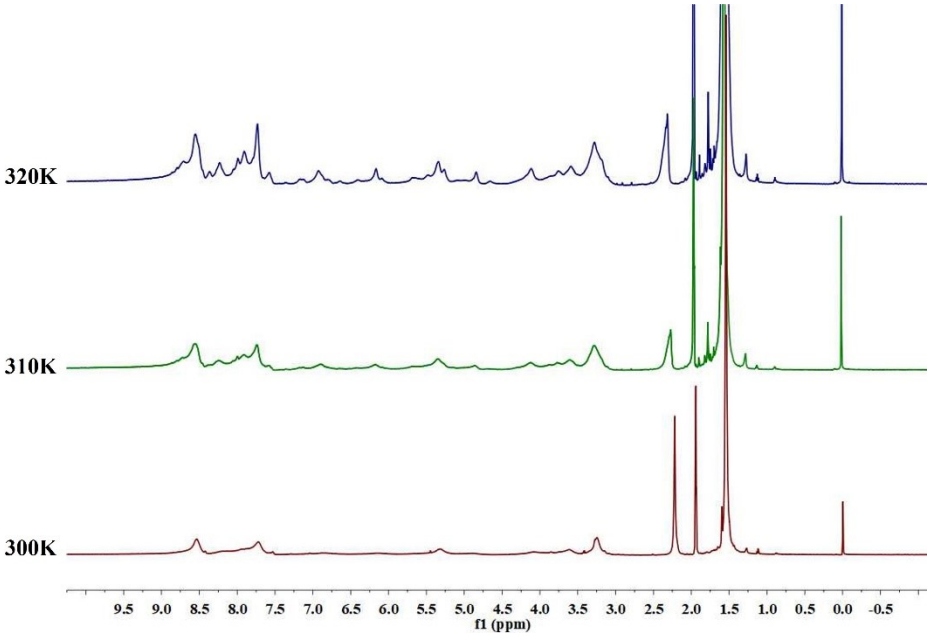

Fig. S12 ^{1}H NMR at different temperatures (600 MHz, CD_3CN, ppm) for **1**.

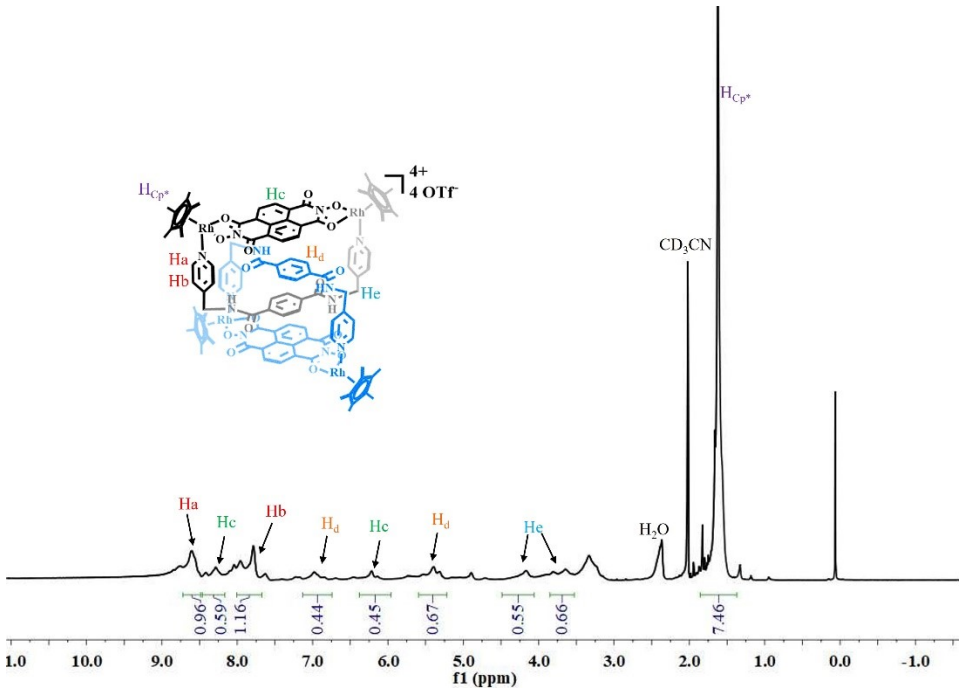

Fig. S13 ^{1}H NMR at 320K (600 MHz, CD_3CN, ppm) for **1**.

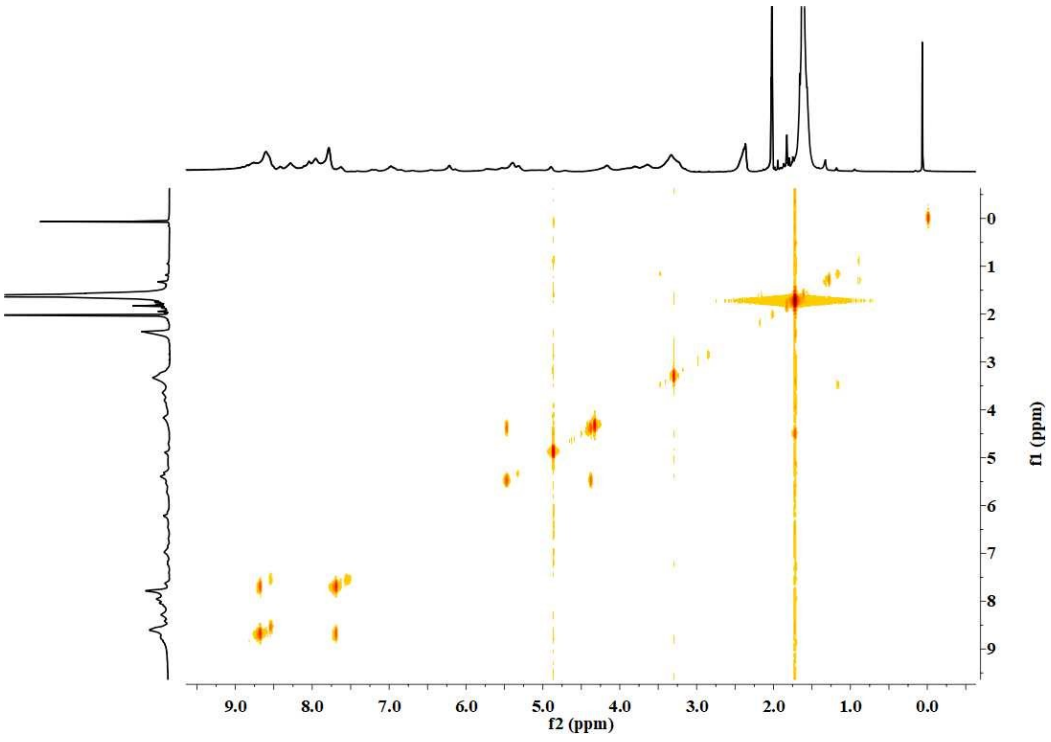

Fig. S14 ^{1}H - ^{1}H COSY NMR spectrum of **1** (600 MHz, CD_3CN) at 320K.

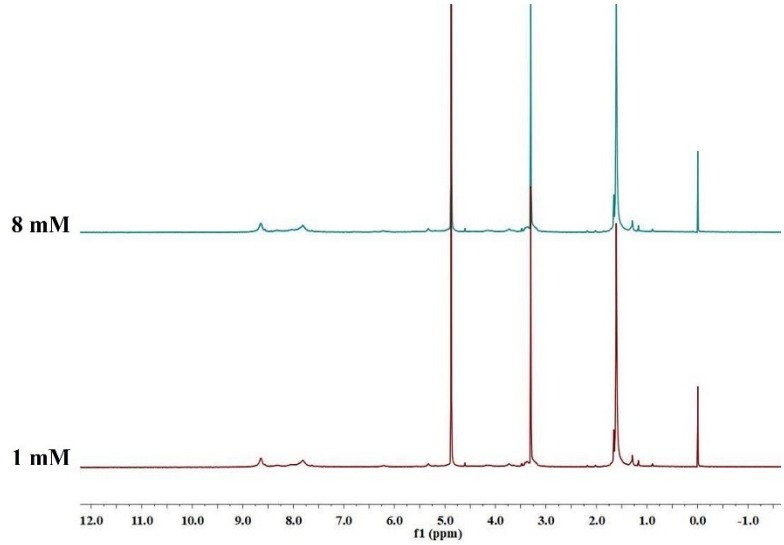

Fig. S15 ^{1}H NMR (600 MHz, CD_3CN, ppm) for **1** at 1mM and 8mM.

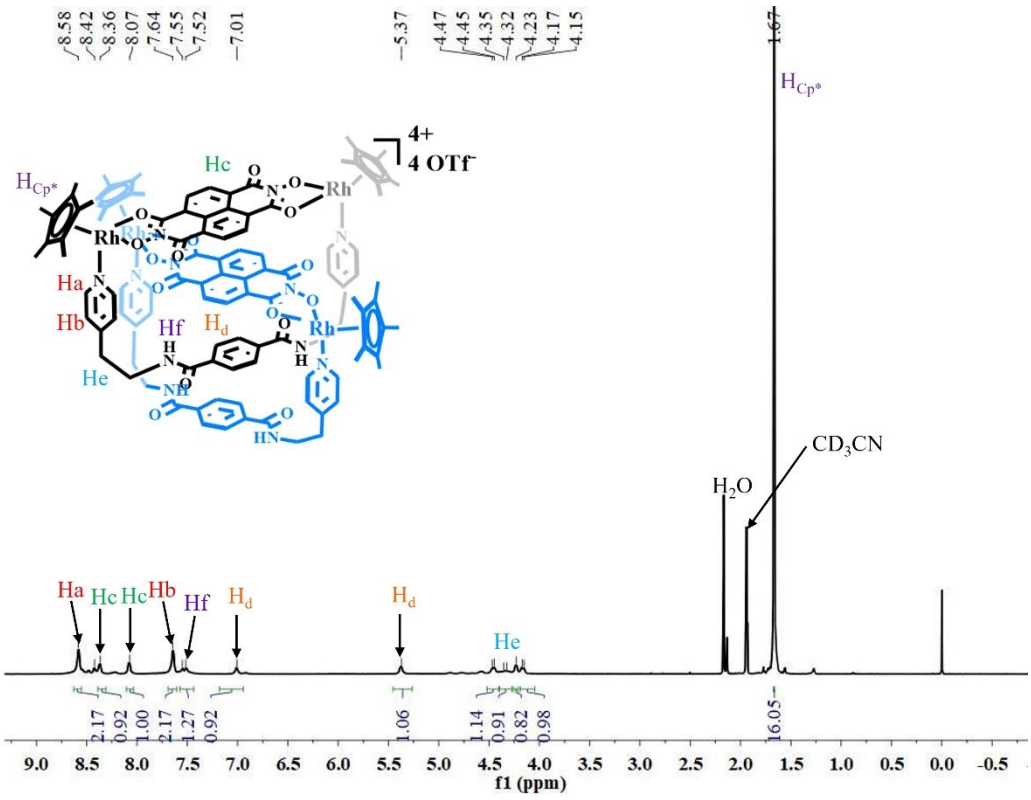

Fig. S16 ^{1}H NMR (600 MHz, CD_3CN, ppm) at 300k for **2**.

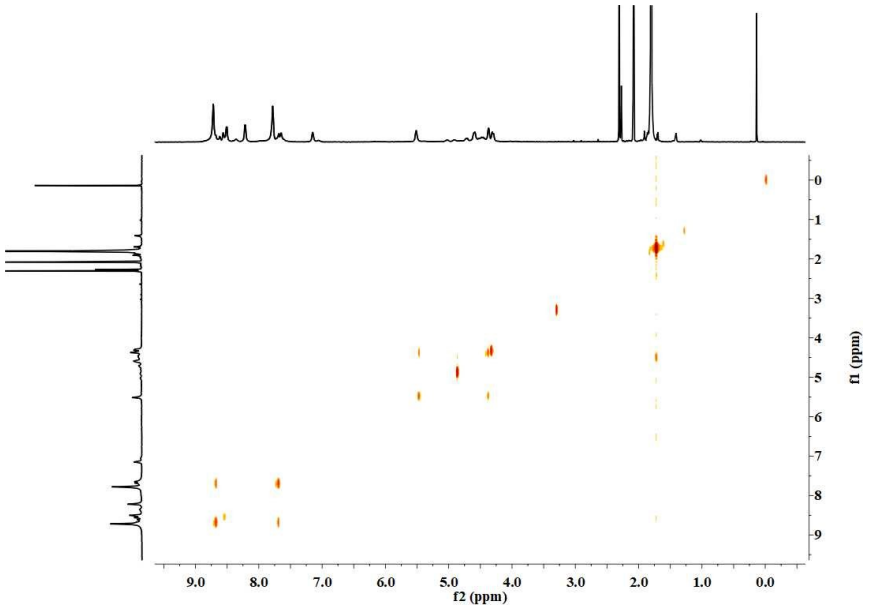

Fig. S17 ^{1}H - ^{1}H COSY NMR spectrum of **2** (600 MHz, CD_3CN, 300K).

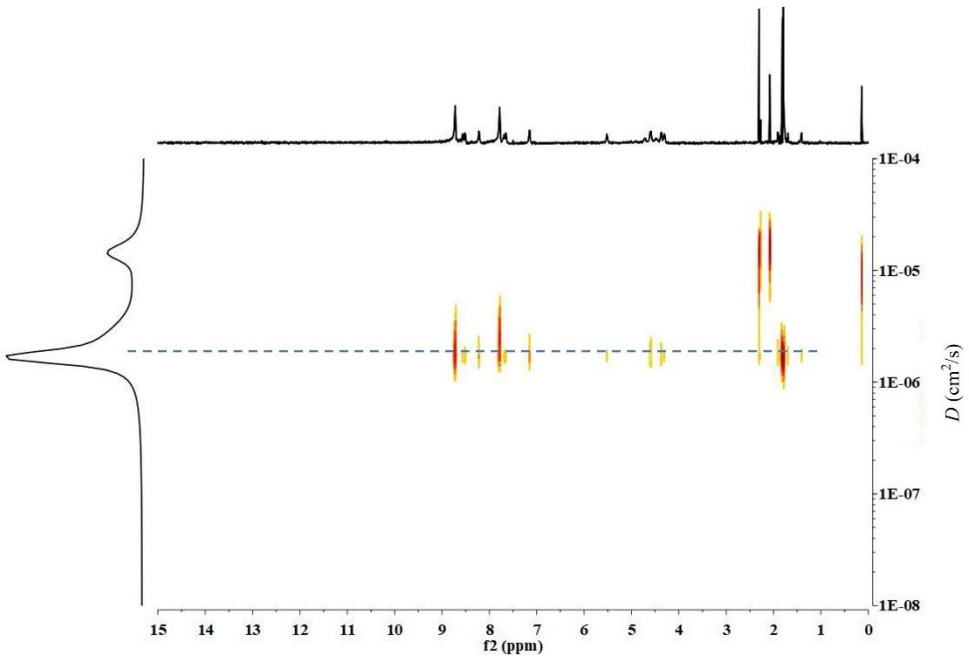

Fig. S18: ^{1}H DOSY NMR spectrum of **2** (600 MHz, CD_3CN, 300K).

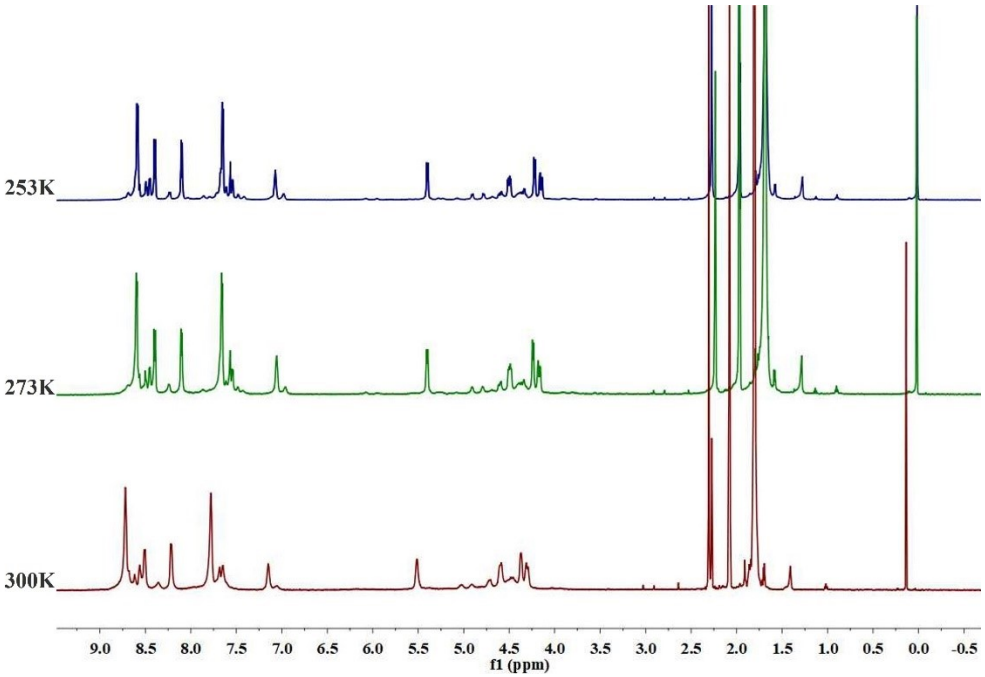

Fig. S19 ^{1}H NMR at different temperatures (600 MHz, CD_3CN, ppm) for **2**.

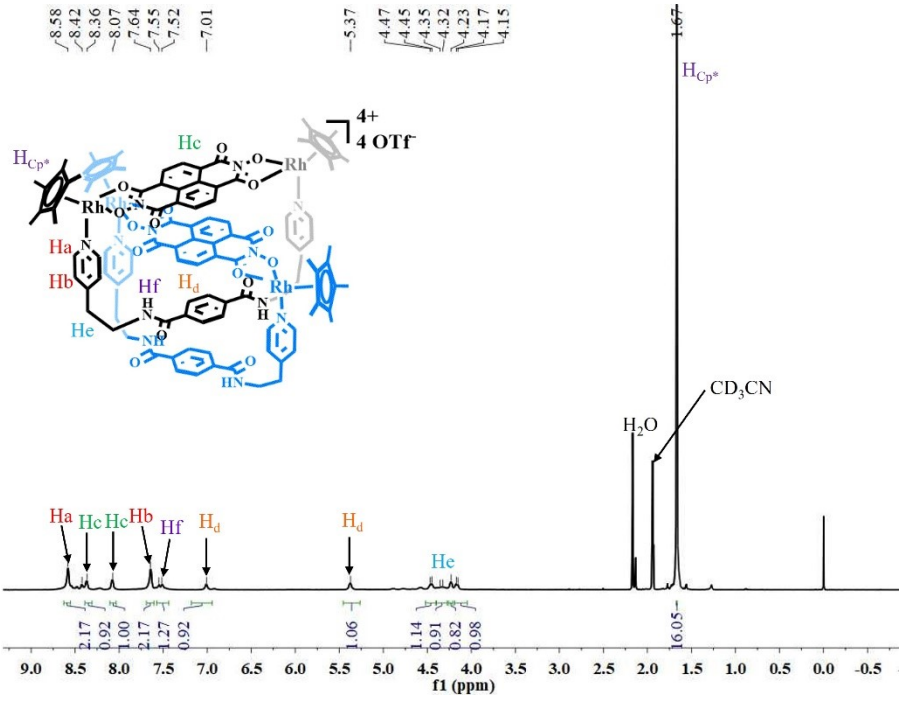

Fig. S20 ^{1}H NMR (600 MHz, CD_3CN, ppm) at 253k for **2**.

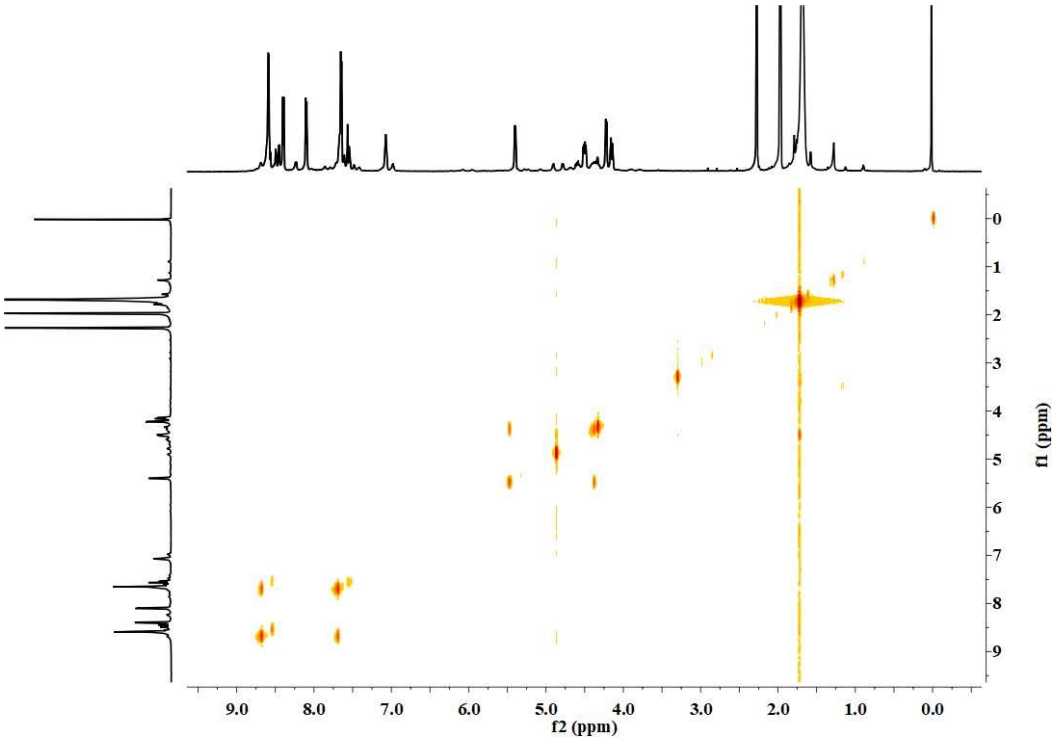

Fig. S21 ^{1}H - ^{1}H COSY NMR spectrum of **2** (600 MHz, CD_3CN, 253K).

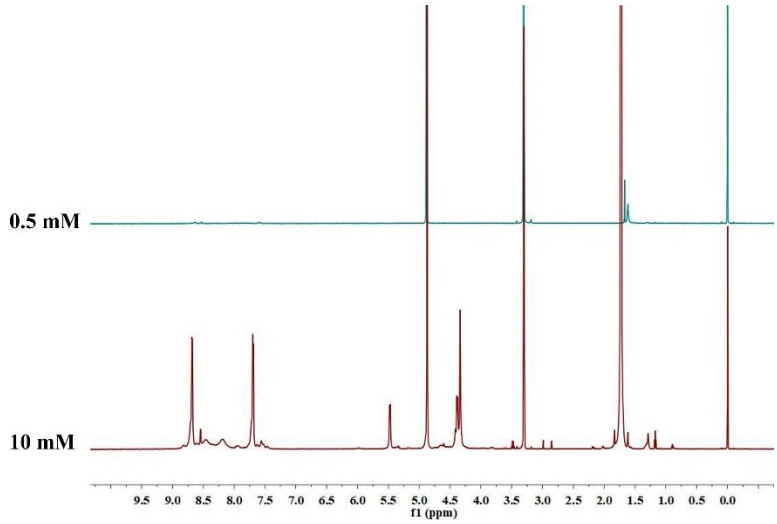

Fig. S22 ^{1}H NMR (600 MHz, CD_3CN, ppm) for **2** at 10mM and 0.5mM.

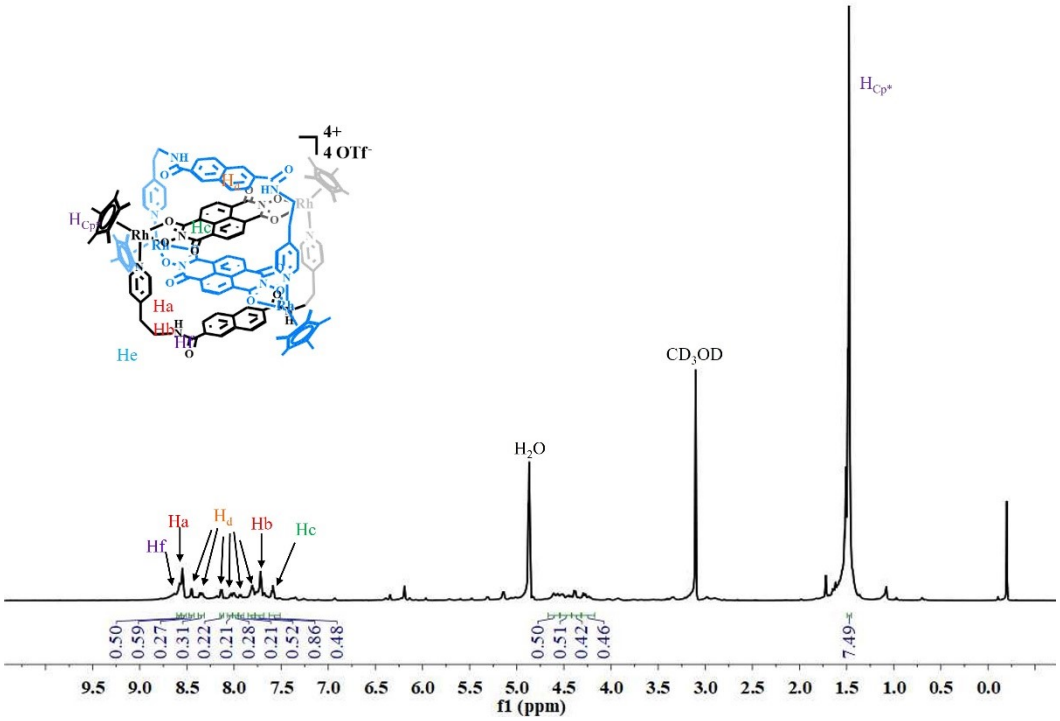

Fig. S23 ^{1}H NMR (600 MHz, CD_3OD, ppm, 300K) for **3**.

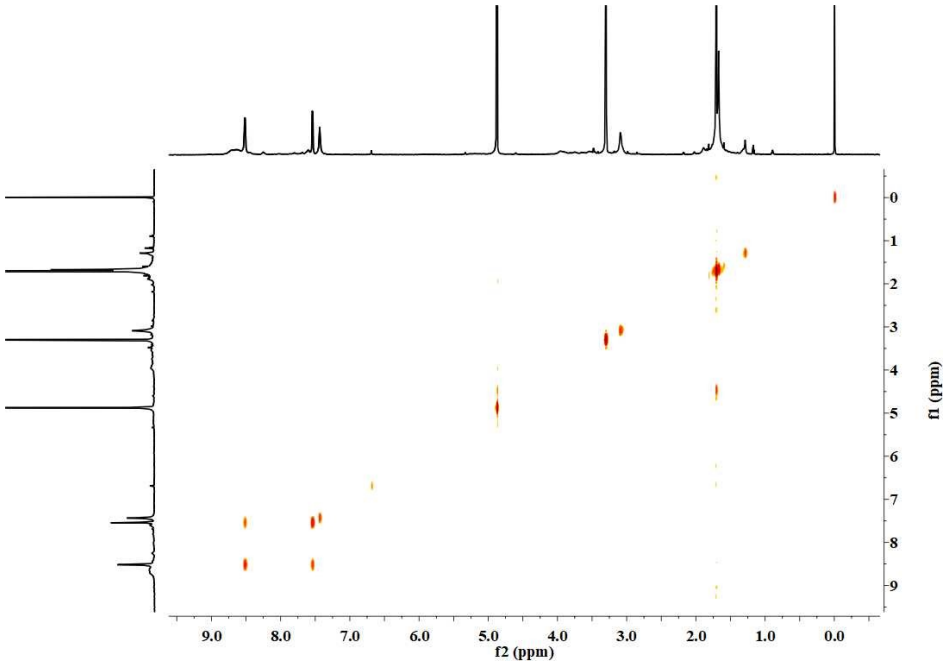

Fig. S24 ^{1}H - ^{1}H COSY NMR spectrum of **3** (600 MHz, CD_3OD, 300K).

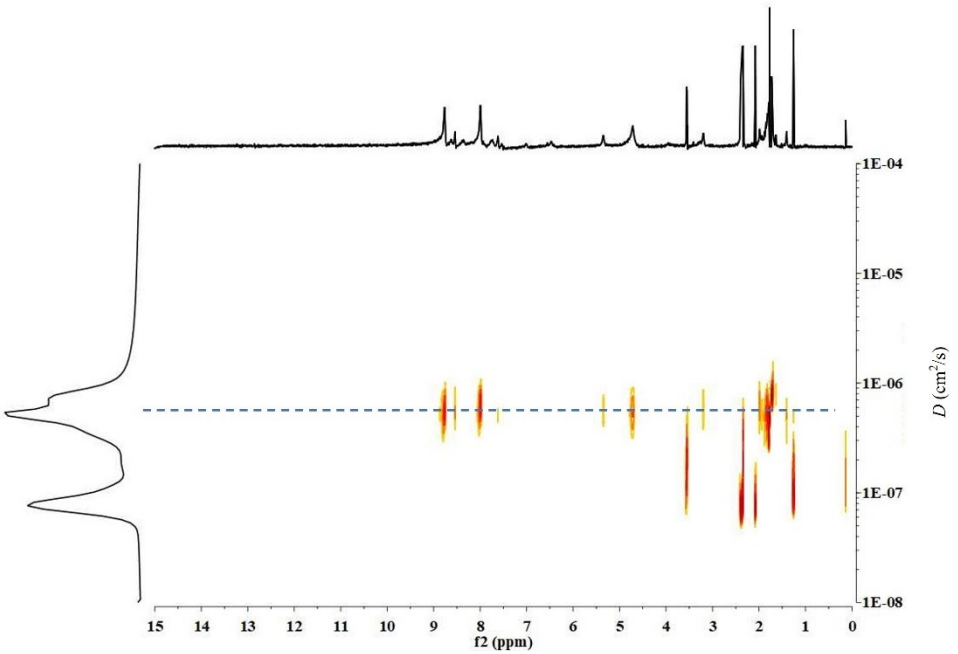

Fig. S25: ^{1}H DOSY NMR spectrum of **3** (600 MHz, CD_3OD, 300k).

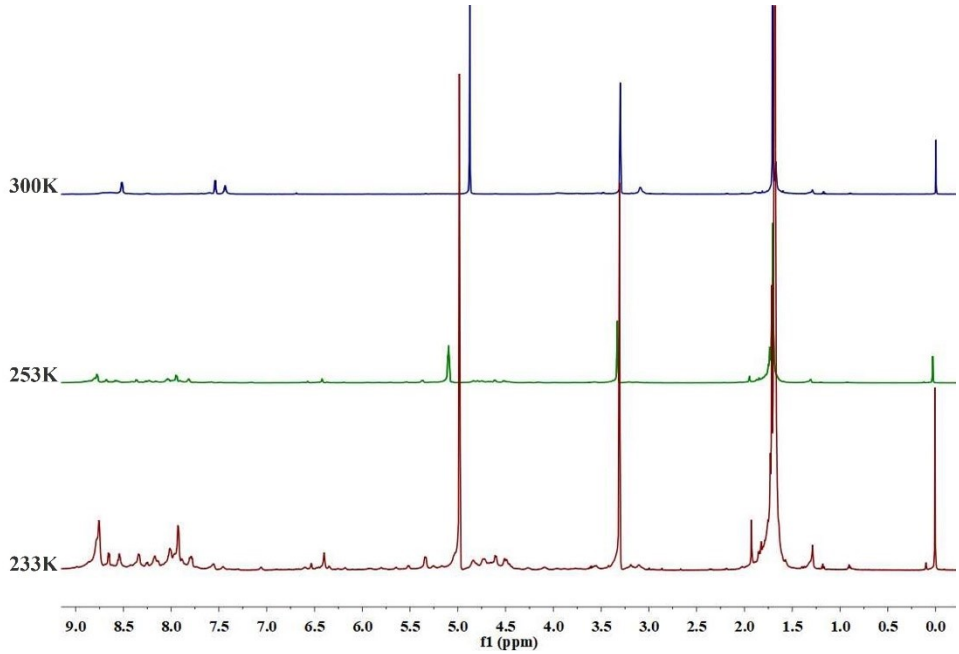

Fig. S26 ^{1}H NMR at different temperatures (600 MHz, CD_3OD, ppm) for **3**.

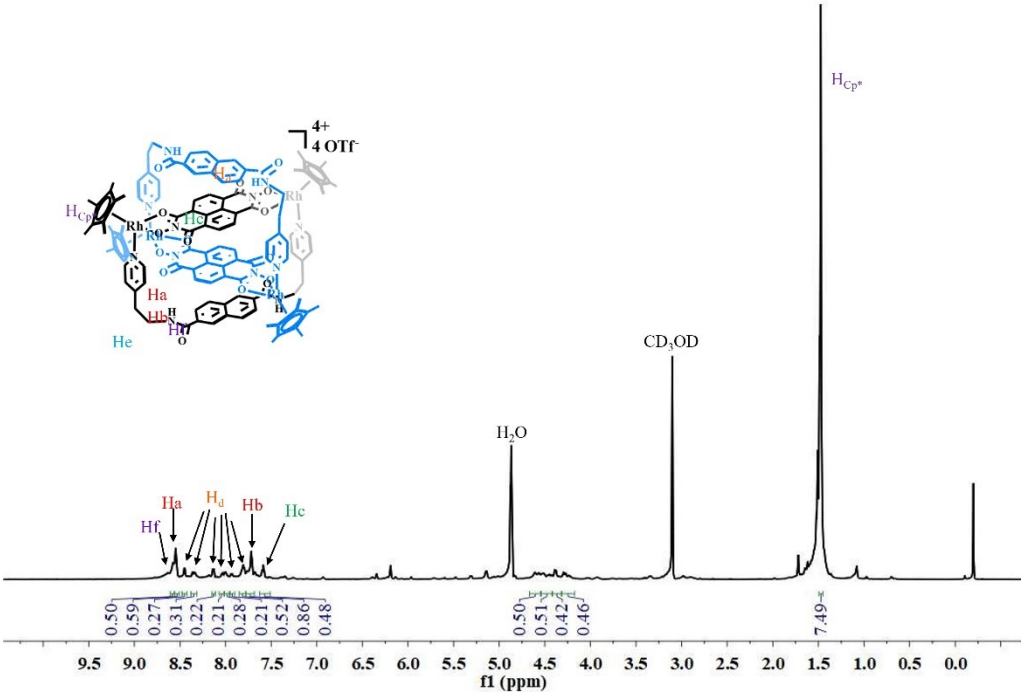

Fig. S27 ^{1}H NMR (600 MHz, CD_3OD, ppm, 233K) for **3**.

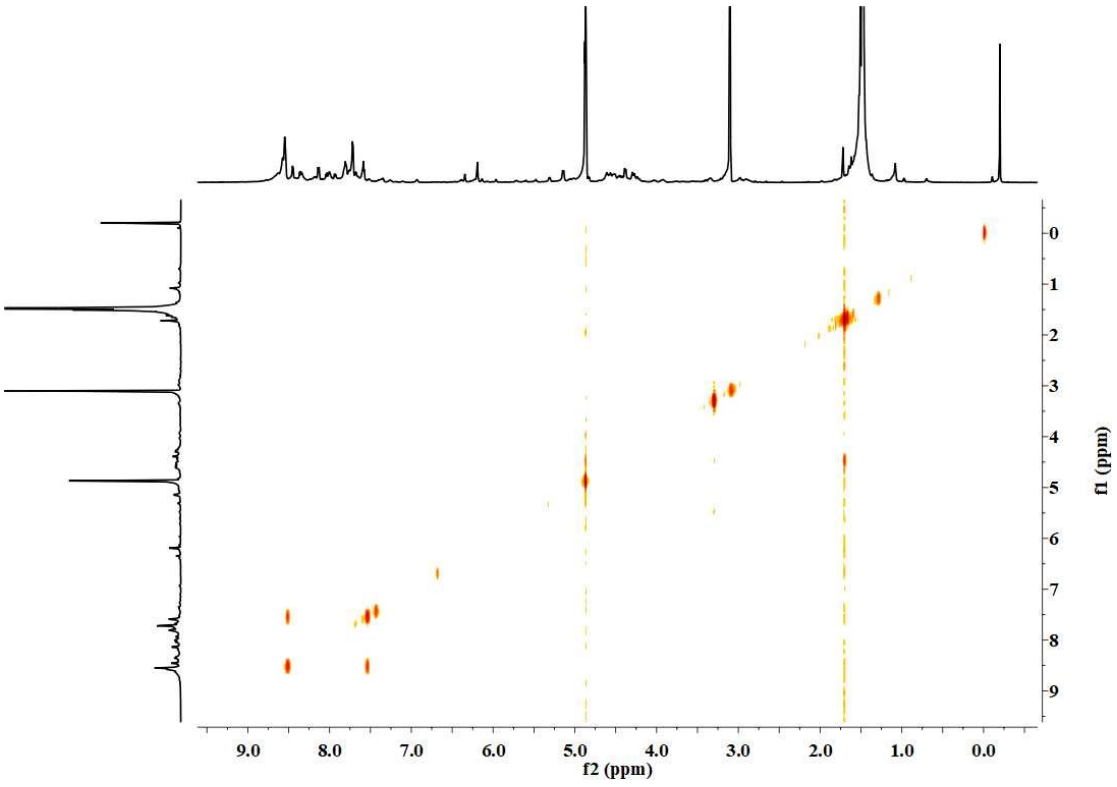

Fig. S28 ^{1}H - ^{1}H COSY NMR spectrum of **3** (600 MHz, CD_3OD, 233K).

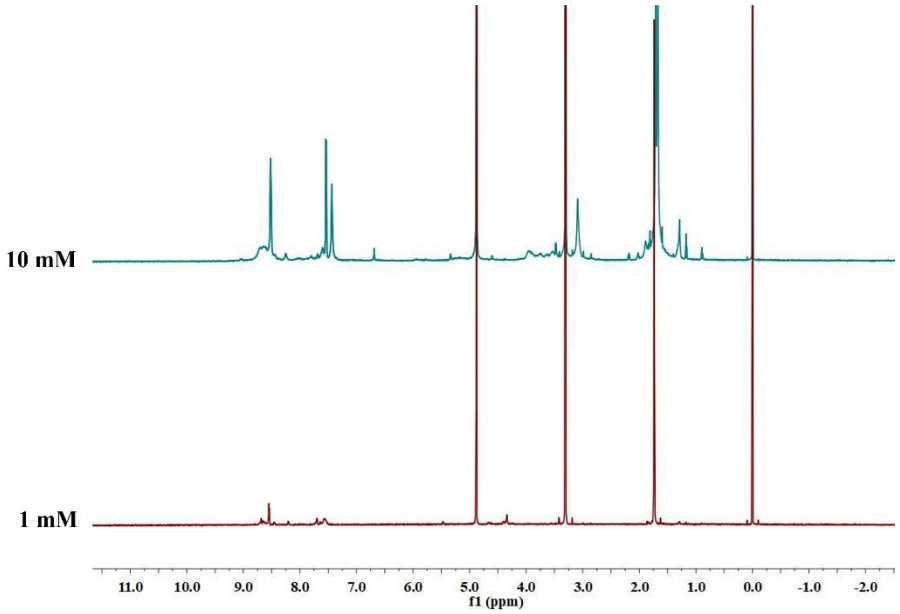

Fig. S29 ^{1}H NMR (600 MHz, CD_3CN, ppm) for **3** at 10mM and 1mM.

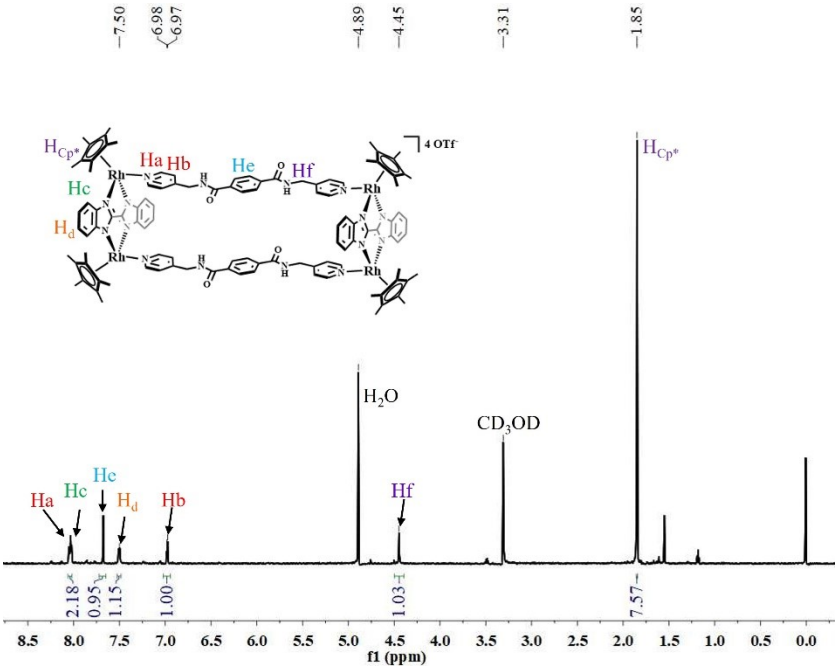

Fig. S30 ^{1}H NMR (600 MHz, CD_3OD, ppm) for **4**.

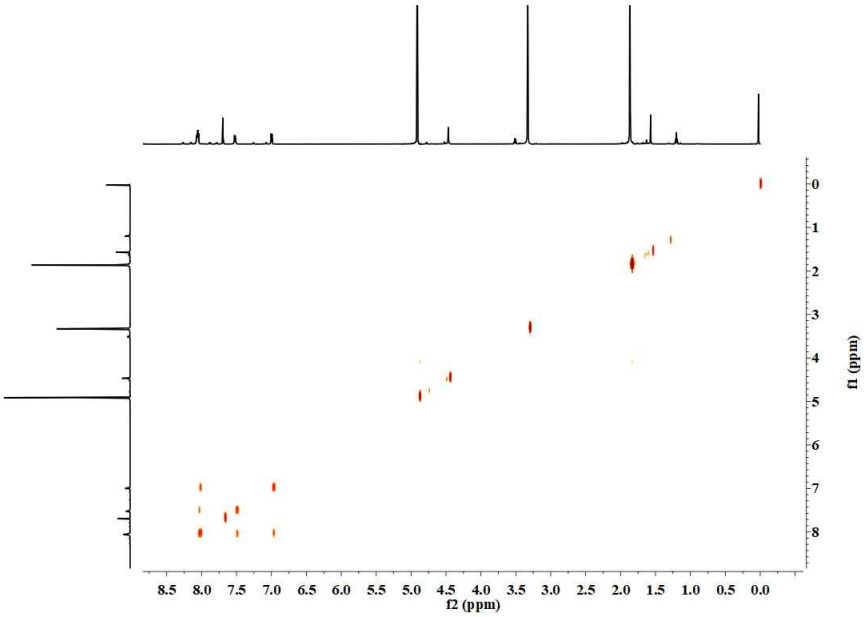

Fig. S31 ^{1}H - ^{1}H COSY NMR spectrum of **4** (600 MHz, CD_3OD).

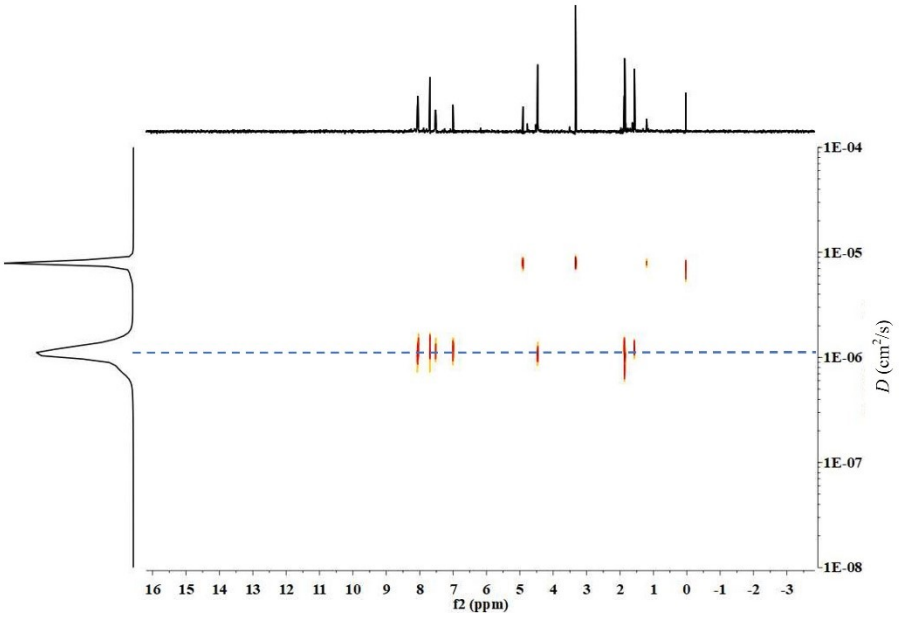

Fig. S32: ^{1}H DOSY NMR spectrum of **4** (600 MHz, CD_3OD).

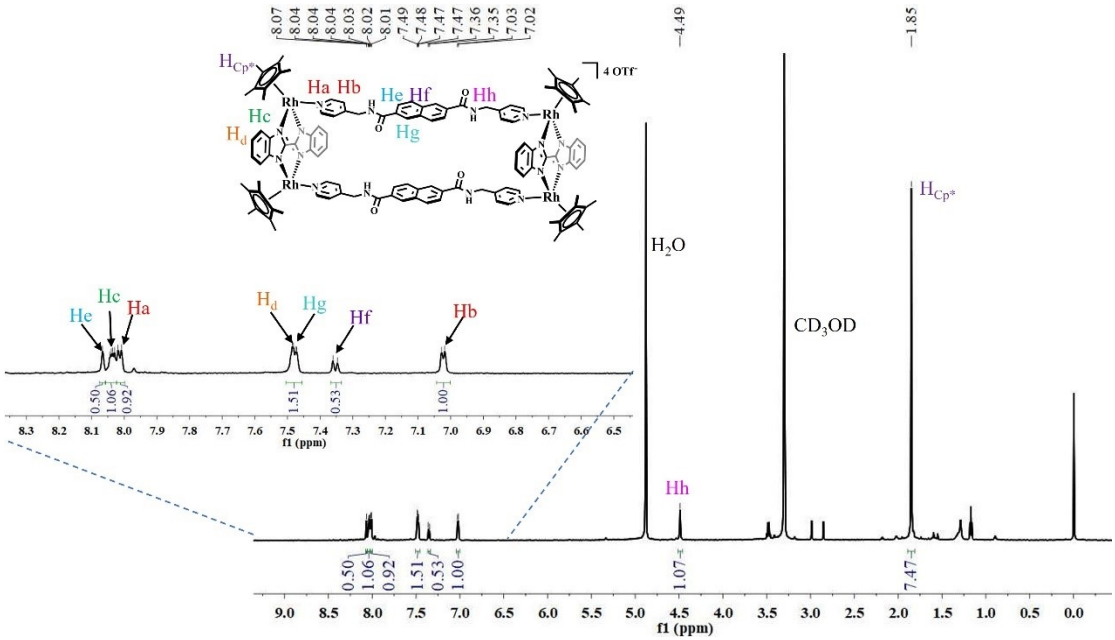

Fig. S33 ^{1}H NMR (600 MHz, CD_3OD, ppm) for **5**.

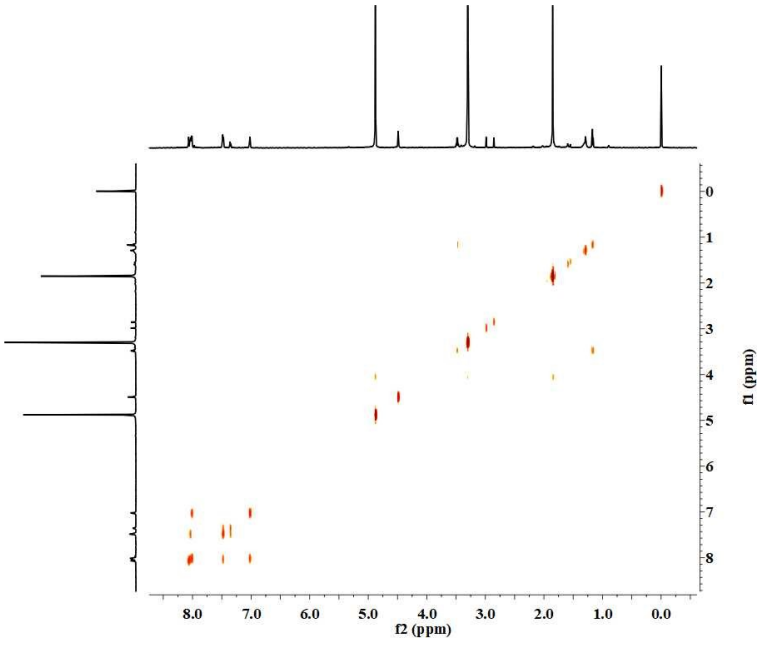

Fig. S34 ^{1}H - ^{1}H COSY NMR spectrum of **5** (600 MHz, CD_3OD).

3. ESI-MS spectra

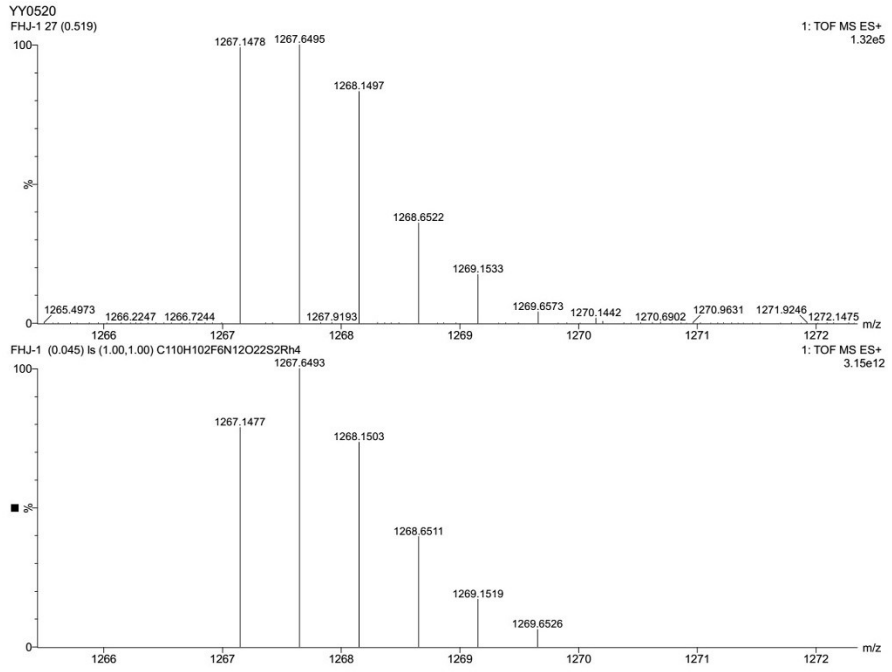

Fig. S35 Experimental (top) and theoretical (bottom) ESI-MS spectra of [**1** – 2OTf$^-$]$^{2+}$.

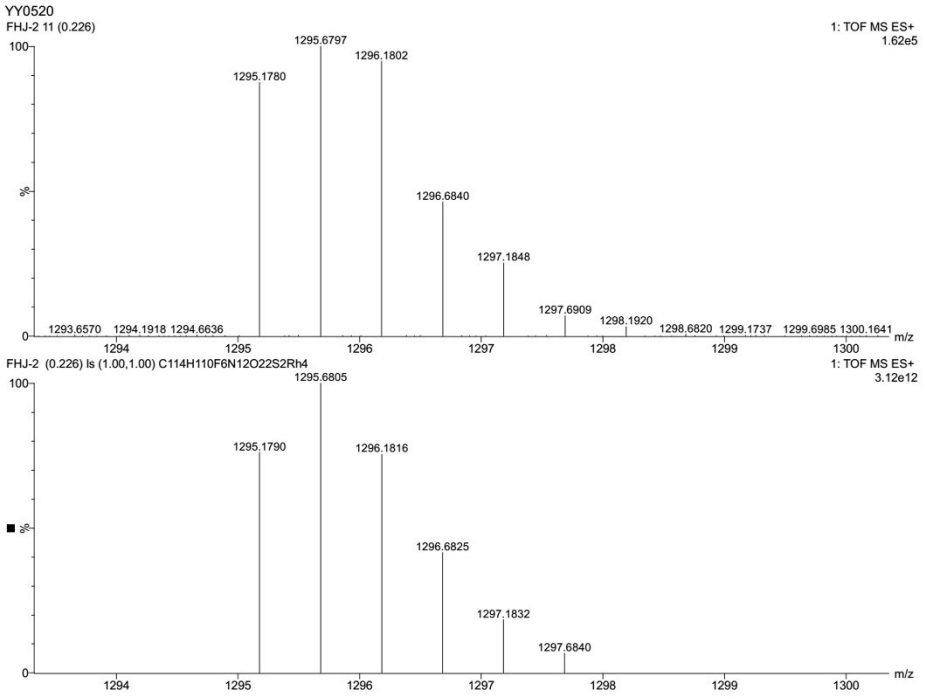

Fig. S36 Experimental (top) and theoretical (bottom) ESI-MS spectra of [**2** – 2OTf$^-$]$^{2+}$.

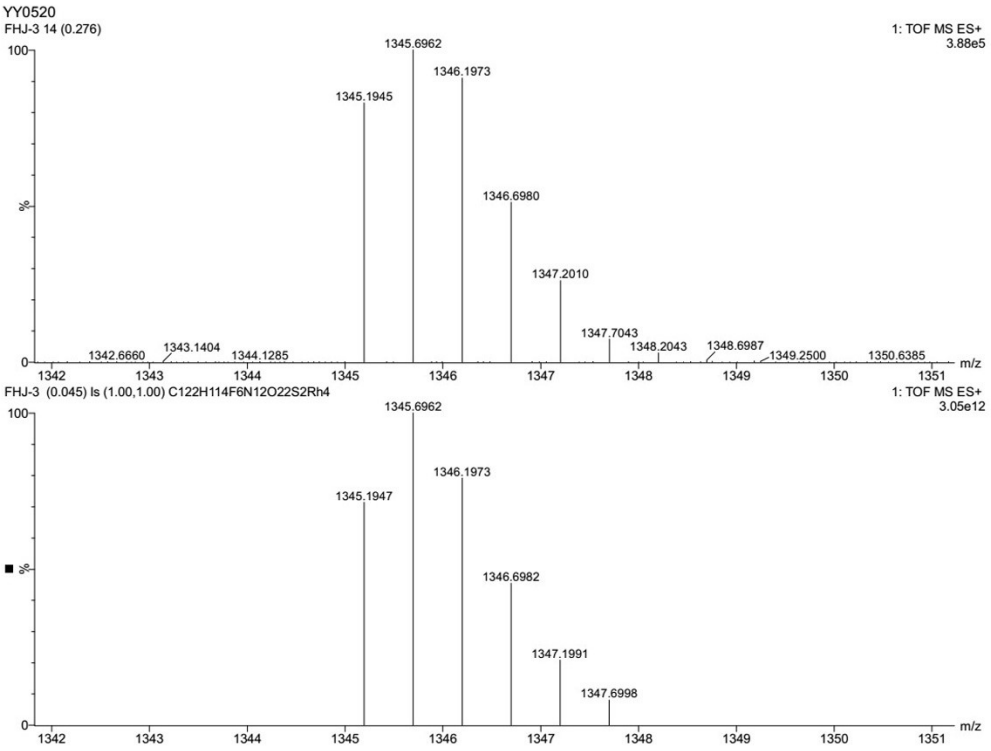

Fig. S37 Experimental (top) and theoretical (bottom) ESI-MS spectra of [**3** – 2OTf$^-$]$^{2+}$.

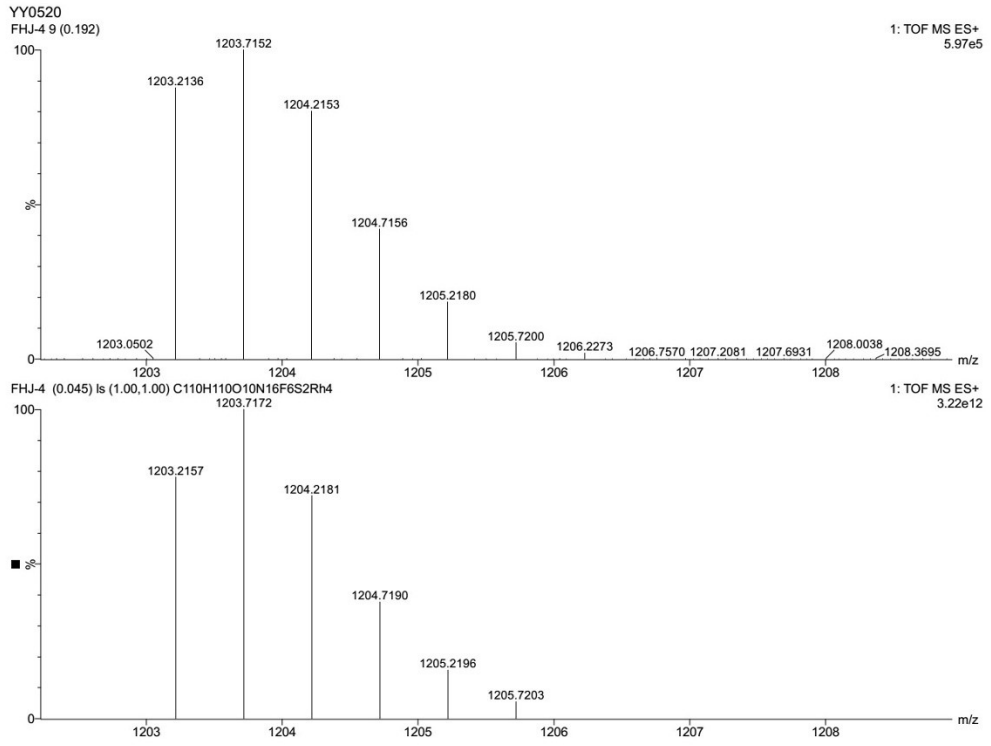

Fig. S38 Experimental (top) and theoretical (bottom) ESI-MS spectra of [**4** – 2OTf$^-$]$^{2+}$.

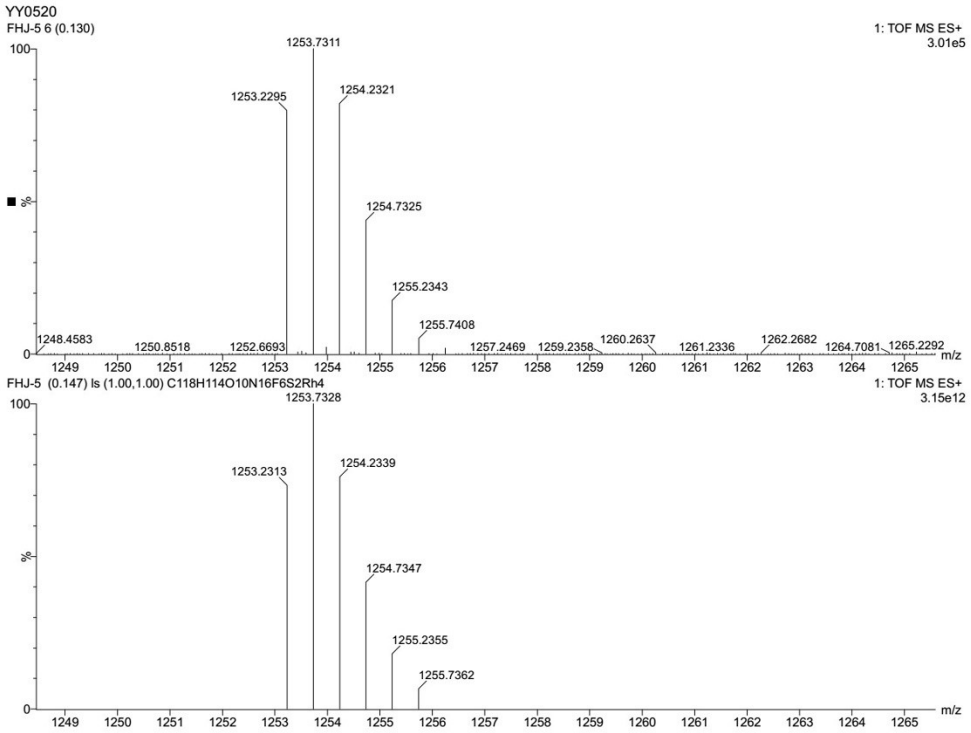

Fig. S39 Experimental (top) and theoretical (bottom) ESI-MS spectra of [**5** – 2OTf$^-$]$^{2+}$.

4. Near-infrared photothermal conversion research:

Experimental details:

To guarantee same amount of conjugated-π area, the applied molar ratio of the five topologies **1** / **2** / **3** / **4** / **5** was 1: 1: 1: 2: 2. Compound **1** (8.5 mg, 0.003mmol) was added into CH_3OH (1.00 ml). After the solid dissolved absolutely, the solution was taken into quartz spectrophotometer cell (1×1×5 cm) and put into the bright spot of a laser with 730 nm wavelength at 0.4 W/cm^2. Temperature variation of the solution was detected by an infrared camera. Compound **2** (8.7 mg, 0.003 mmol), compound **3** (8.9 mg, 0.003 mmol), Compound **4** (16.2 mg, 0.003 mmol) and compound **5** (16.8 mg, 0.006 mmol) were detected with the same procedure as compound **1**.

Equations used to calculate near-infrared photothermal conversion efficiency were exhibited as follows:

$$\eta = hS(\Delta T_{sample} - \Delta T_{solvent}) / I(1\text{-}10^{-A}) \quad \textbf{(1)}$$

$$hS = \sum mC_p / \tau_s \quad \textbf{(2)}$$

$$\tau_s = -t / \ln\theta \quad \textbf{(3)}$$

$$\theta = (T_{amb} - T) / (T_{amb} - T_{max}) \quad \textbf{(4)}$$

$\sum mC_p$ = m(methanol)·Cp(methanol) = ρ(methanol)·V(methanol)·Cp(methanol) = 0.777×1.0×2.51 = 1.9503 J·K^{-1}. $\Delta T_{solvent}$ = 2.0 ℃. I = 0.4 W/cm^2.

In the equations 1-4 provided above, h represents the heat transfer coefficient, while S stands for the surface area of the container. τ_s denotes the time constant of the sample system, m indicates the mass of the products, and Cp signifies the specific heat capacity of the solvent.

(1) [2]-catenane **1** (**B–L–L–B**).

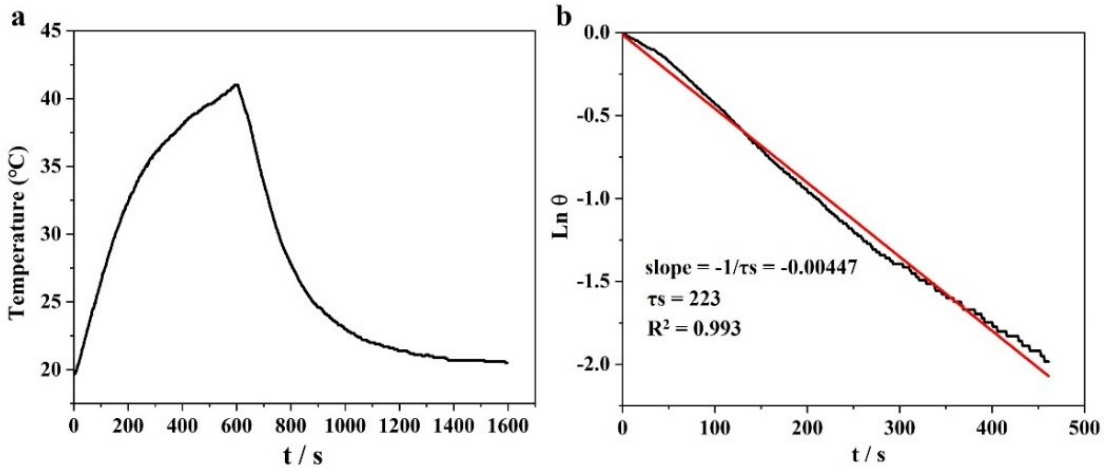

Fig. S40 (a) Heating and cooling curve of [2]-catenane **1** (with B–L–L–B stacking). (b) Fitting linear of lnθ-t.

Near-infrared photothermal conversion efficiency η of **1** was calculated by equations above. A fitting linear of lnθ-t was obtained by Eqs (**3**) and (**4**), by which τ_s was calculated as 223 s. Thus, $hS = 1.9503 / 223 = 8.7457 \times 10^{-3}$ J·K^{-1}·S^{-1}. ΔTsample = 21.3 °C (41.0 – 19.7, Fig. S26a). A1 = 0.5755 (Fig.5b in main text). Eventually, $\eta 1 = 8.7457 \times 10^{-3} \times (21.3 - 2.0) / [0.4 \times (1 - 10^{-0.5755}) = 57.0\%$.

(2) [2]-catenane **2** (**B–B–L–L**).

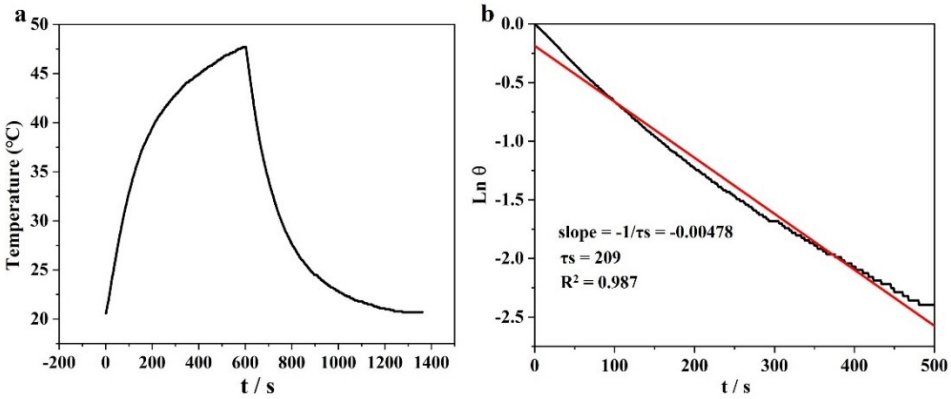

Fig. S41 (a) Heating and cooling curve of [2]-catenane **2** (with B–B–L–L stacking). (b) Fitting linear of lnθ-t.

Near-infrared photothermal conversion efficiency η of **2** was calculated by equations above. A fitting linear of lnθ-t was obtained by Eqs (**3**) and (**4**), by which τ_s was calculated as 209 s. Thus, $hS = 1.9503 / 209 = 9.3316 \times 10^{-3}$ J·K^{-1}·S^{-1}. ΔTsample = 27.1 °C (47.7 – 20.6, Fig. S27a). A1 = 0.6571 (Fig.5b in main text). Eventually, $\eta 2 = 9.3316 \times 10^{-3} \times (27.1 - 2.0) / [0.4 \times (1 - 10^{-0.6571}) = 75.0\%$.

(3) [2]-catenane **3** (**L–B–B–L**).

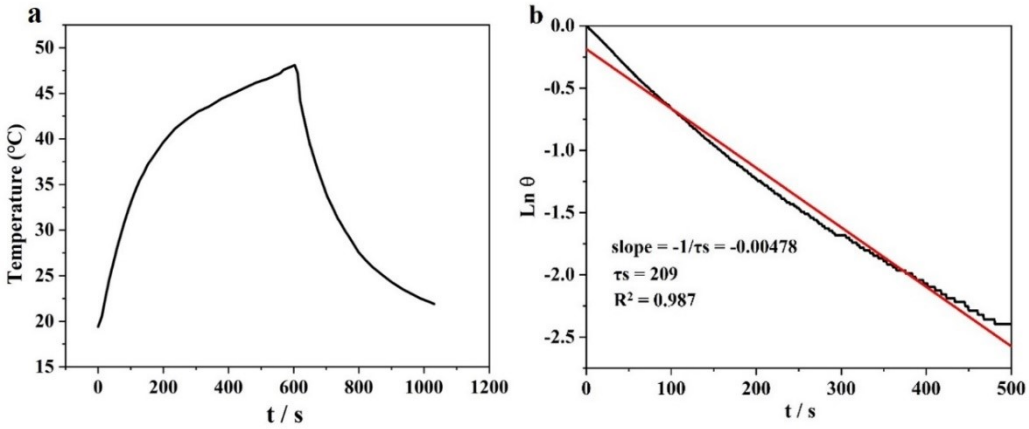

Fig. S42 (a) Heating and cooling curve of [2]-catenane **3** (with L–B–B–L stacking). (b) Fitting linear of lnθ-t.

Near-infrared photothermal conversion efficiency η of **3** was calculated by equations above. A fitting linear of lnθ-t was obtained by Eqs (**3**) and (**4**), by which τ_s was calculated as 193 s. Thus, hS = 1.9503 / 193 = 10.1052 × 10^{-3} J·K^{-1}·S^{-1}. ΔTsample = 27.6 ℃ (48.1 – 20.5, Fig. S28a). A1 = 0.6443 (Fig.5b in main text). Eventually, $\eta 2$ = 10.1052 × 10^{-3} × (27.6 – 2.0) / [0.4 × (1 – $10^{-0.6443}$) = 83.7%.

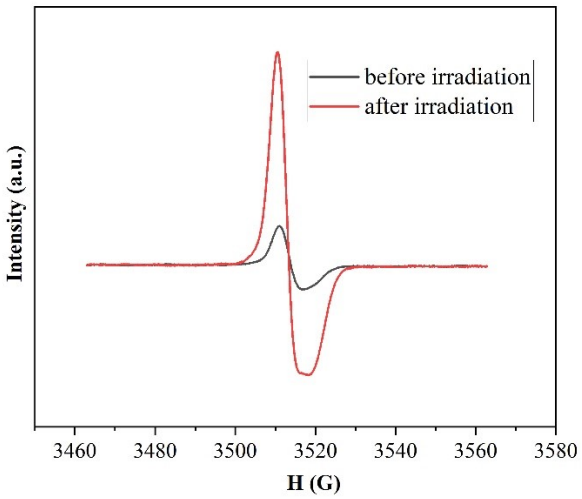

Fig. S43 EPR spectra of [2]-catenane **1** before and after irradiation.

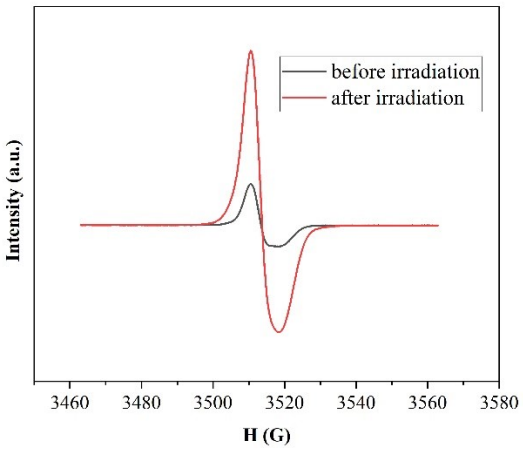

Fig. S44 EPR spectra of [2]-catenane **2** before and after irradiation.

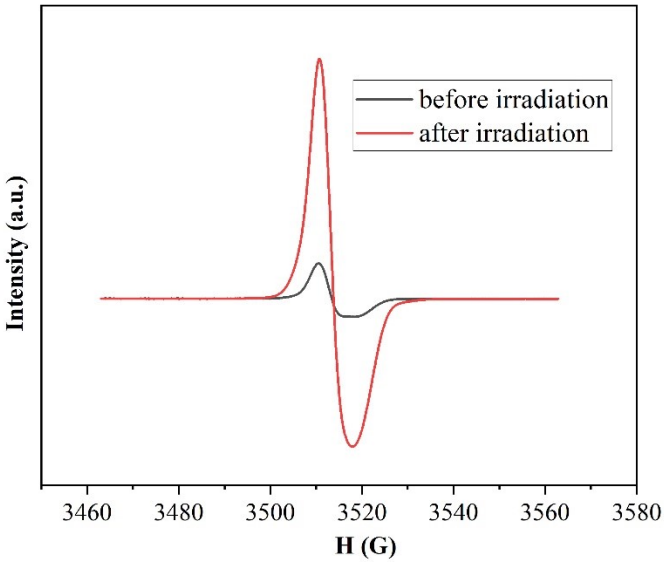

Fig. S45 EPR spectra of [2]-catenane **3** before and after irradiation.

5. X-ray crystallography details

X-ray Crystallography Details. Single crystals of **1**, **2**, **3**, **4** and **5** suitable for X-ray diffraction study were obtained at room temperature. Crystallographic data for complexes **1**, **2**, **3**, **4** and **5** were collected at 173 K with a Bruker D8 VENTURE microfocus X-ray source system (Cu Ka, l = 1.54178 A˚).

In asymmetric unit of **1**, a solvent mask was calculated and 650 electrons were found in a volume of 2674\%A^3^ in 2 voids per unit cell. This is consistent with the presence of 1[CH_3OH], 8[CH_3OH] per Asymmetric Unit which account for 648 electrons per unit cell.

In asymmetric unit of **2**, a solvent mask was calculated and 534 electrons were found in a volume of 1464\%A^3^ in 3 voids per unit cell. This is consistent with the presence of 6[CH_3OH], 1[H_2O], 1[H_2O] per Asymmetric Unit which account for 512 electrons per unit cell.

In asymmetric unit of **3**, a solvent mask was calculated and 250 electrons were found in a volume of 792\%A^3^ in 2 voids per unit cell. This is consistent with the presence of 1[C_3H_7NO], 1[CH_3OH] per Asymmetric Unit which account for 232 electrons per unit cell.

In asymmetric unit of **4**, a solvent mask was calculated and 114 electrons were found in a volume of 443\%A^3^ in 3 voids per unit cell. This is consistent with the presence of 2[C_3H_7NO], 2.8[H_2O] per Asymmetric Unit which account for 108 electrons per unit cell.

In asymmetric unit of **5**, a solvent mask was calculated and 829 electrons were found in a volume of 1976\%A^3^ in 1 void per unit cell. This is consistent with the presence of 22[CH_3OH] per Asymmetric Unit which account for 792 electrons per unit cell.

Table S1. Crystal data for complex **1**.

Complex	**1**
Empirical formula	$C_{121}H_{140}F_{12}N_{12}O_{37}Rh_4S_4$
Formula weight	3122.32
Temperature	173.00 K
Wavelength	1.34138 Å
Crystal system	Monoclinic
Space group	P 1 21/n 1
Unit cell dimensions	a = 13.9735(8) Å
	b = 53.355(3) Å
	c = 17.4998(10) Å
Volume	13039.4(13) $Å^3$
Z	4
Density (calculated)	1.590 Mg/m^3
Absorption coefficient	3.689 mm^{-1}
F(000)	6392
Crystal size	0.3 x 0.2 x 0.2 mm^3
Theta range for data collection	2.628 to 54.959°.
Index ranges	-16<=h<=17, -65<=k<=64, -21<=l<=21
Reflections collected	87383
Independent reflections	24709 [R(int) = 0.0503]
Completeness to theta = 53.594°	99.7 %
Absorption correction	Semi-empirical from equivalents
Max. and min. transmission	0.7508 and 0.4981
Refinement method	Full-matrix least-squares on F^2
Data / restraints / parameters	24709 / 1752 / 1569
Goodness-of-fit on F^2	1.027
Final R indices [I>2sigma(I)]	R1 = 0.0693, wR2 = 0.1839
R indices (all data)	R1 = 0.0881, wR2 = 0.1988
Extinction coefficient	n/a
Largest diff. peak and hole	1.907 and -1.725 e.$Å^{-3}$

[α]：$R_1=\Sigma||F_0|-|F_c||/\Sigma|F_0|$ (based on reflections with $F_0^2>2\sigma F^2$). $wR_2=[\Sigma[w(F_0^2-F_c^2)^2]/\Sigma[w(F_0^2)^2]]^{1/2}$; $w=1/[\sigma^2(F_0^2)+(0.095P)^2]$; $P=[\max(F_0^2, 0)+2F_c^2]/3(F_0^2>2\sigma F^2)$.

Table S2. Crystal data for complex **2**.

Complex	**2**
Empirical formula	$C_{125}H_{151}F_{12}N_{12}O_{39}Rh_4S_4$
Formula weight	3213.45
Temperature	173.00 K
Wavelength	1.34139 Å
Crystal system	Monoclinic
Space group	P 1 21/c 1
Unit cell dimensions	a = 22.9933(18) Å
	b = 21.6473(17) Å
	c = 26.969(2) Å
Volume	13236.0(18) $Å^3$
Z	4
Density (calculated)	1.613 Mg/m^3
Absorption coefficient	3.653 mm^{-1}
F(000)	6596
Crystal size	0.3 x 0.3 x 0.1 mm^3
Theta range for data collection	2.702 to 53.326°.
Index ranges	-27<=h<=26, -20<=k<=25, -31<=l<=31
Reflections collected	101492
Independent reflections	23323 [R(int) = 0.1191]
Completeness to theta = 53.326°	98.4 %
Absorption correction	Semi-empirical from equivalents
Max. and min. transmission	0.7504 and 0.2686
Refinement method	Full-matrix least-squares on F^2
Data / restraints / parameters	23323 / 1871 / 1613
Goodness-of-fit on F^2	1.111
Final R indices [I>2sigma(I)]	R1 = 0.1325, wR2 = 0.2618
R indices (all data)	R1 = 0.1741, wR2 = 0.2817
Extinction coefficient	n/a
Largest diff. peak and hole	2.433 and -1.537 $e.Å^{-3}$

[α]：$R_1=\Sigma||F_0|-|F_c||/\Sigma|F_0|$ (based on reflections with $F_0^2>2\sigma F^2$). $wR_2=[\Sigma[w(F_0^2-F_c^2)^2]/\Sigma[w(F_0^2)^2]]^{1/2}$; $w=1/[\sigma^2(F_0^2)+(0.095P)^2]$; $P=[\max(F_0^2, 0)+2F_c^2]/3(F_0^2>2\sigma F^2)$.

Table S3. Crystal data for complex **3**.

Complex	**3**
Empirical formula	$C_{67}H_{73}F_6N_7O_{15.63}Rh_2S_2$
Formula weight	1610.32
Temperature	173.00 K
Wavelength	1.34139 Å
Crystal system	Orthorhombic
Space group	$P2_12_12$
Unit cell dimensions	a = 28.7856(8) Å
	b = 14.4874(4) Å
	c = 15.6484(4) Å
Volume	6525.8(3) $Å^3$
Z	4
Density (calculated)	1.639 Mg/m^3
Absorption coefficient	3.681 mm^{-1}
F(000)	3300
Crystal size	0.21 x 0.19 x 0.17 mm^3
Theta range for data collection	2.971 to 52.982°.
Index ranges	-34<=h<=34, -17<=k<=15, -18<=l<=18
Reflections collected	53732
Independent reflections	11508 [R(int) = 0.0544]
Completeness to theta = 52.982°	99.8 %
Absorption correction	Semi-empirical from equivalents
Max. and min. transmission	0.7512 and 0.3544
Refinement method	Full-matrix least-squares on F^2
Data / restraints / parameters	11508 / 926 / 859
Goodness-of-fit on F^2	1.038
Final R indices [I>2sigma(I)]	R1 = 0.0656, wR2 = 0.1737
R indices (all data)	R1 = 0.0759, wR2 = 0.1853
Absolute structure parameter	0.47(2)
Extinction coefficient	n/a
Largest diff. peak and hole	1.181 and -1.583 e.$Å^{-3}$

[α]：$R_1=\Sigma||F_0|-|F_c||/\Sigma|F_0|$ (based on reflections with $F_0^2>2\sigma F^2$). $wR_2=[\Sigma[w(F_0^2-F_c^2)^2]/\Sigma[w(F_0^2)^2]]^{1/2}$; $w=1/[\sigma^2(F_0^2)+(0.095P)^2]$; $P=[\max(F_0^2, 0)+2F_c^2]/3(F_0^2>2\sigma F^2)$.

Table S4. Crystal data for complex **4**.

Complex	**4**
Empirical formula	$C_{118}H_{131.60}F_{12}N_{18}O_{20.80}Rh_4S_4$
Formula weight	2902.68
Temperature	173.00 K
Wavelength	1.34139 Å
Crystal system	Triclinic
Space group	P-1
Unit cell dimensions	a = 12.7842(9) Å
	b = 13.3300(10) Å
	c = 20.9500(15) Å
Volume	3148.9(4) $Å^3$
Z	1
Density (calculated)	1.531 Mg/m^3
Absorption coefficient	3.728 mm^{-1}
F(000)	1484
Crystal size	0.2 x 0.2 x 0.2 mm^3
Theta range for data collection	3.114 to 55.104°.
Index ranges	-15<=h<=14, -16<=k<=16, -25<=l<=25
Reflections collected	28559
Independent reflections	11723 [R(int) = 0.0788]
Completeness to theta = 53.594°	98.1 %
Absorption correction	Semi-empirical from equivalents
Max. and min. transmission	0.7508 and 0.2888
Refinement method	Full-matrix least-squares on F^2
Data / restraints / parameters	11723 / 803 / 763
Goodness-of-fit on F^2	1.059
Final R indices [I>2sigma(I)]	R1 = 0.1046, wR2 = 0.2091
R indices (all data)	R1 = 0.1528, wR2 = 0.2365
Extinction coefficient	n/a
Largest diff. peak and hole	2.094 and -1.821 e.$Å^{-3}$

[α]：$R_1=\Sigma||F_0|-|F_c||/\Sigma|F_0|$ (based on reflections with $F_0^2>2\sigma F^2$). $wR_2=[\Sigma[w(F_0^2-F_c^2)^2]/\Sigma[w(F_0^2)^2]]^{1/2}$; $w=1/[\sigma^2(F_0^2)+(0.095P)^2]$; $P=[\max(F_0^2, 0)+2F_c^2]/3(F_0^2>2\sigma F^2)$.

Table S5. Crystal data for complex **5**.

Complex	**5**
Empirical formula	$C_{140}H_{204}F_6N_{16}O_{32}Rh_4S_2$
Formula weight	3212.94
Temperature	173.00 K
Wavelength	1.34139 Å
Crystal system	Monoclinic
Space group	P 1 21/n 1
Unit cell dimensions	a = 13.7998(11) Å
	b = 32.678(3) Å
	c = 16.4748(13) Å
Volume	6898.8(10) $Å^3$
Z	2
Density (calculated)	1.547 Mg/m^3
Absorption coefficient	3.254 mm^{-1}
F(000)	3356
Crystal size	0.19 x 0.17 x 0.15 mm^3
Theta range for data collection	3.223 to 52.093°.
Index ranges	-16<=h<=16, -38<=k<=38, -19<=l<=15
Reflections collected	48986
Independent reflections	11647 [R(int) = 0.0585]
Completeness to theta = 52.093°	99.0 %
Absorption correction	Semi-empirical from equivalents
Max. and min. transmission	0.7505 and 0.3635
Refinement method	Full-matrix least-squares on F^2
Data / restraints / parameters	11647 / 878 / 713
Goodness-of-fit on F^2	1.068
Final R indices [I>2sigma(I)]	R1 = 0.1007, wR2 = 0.2014
R indices (all data)	R1 = 0.1260, wR2 = 0.2172
Extinction coefficient	n/a
Largest diff. peak and hole	2.611 and -1.519 e.$Å^{-3}$

[α]：$R_1=\Sigma||F_0|-|F_c||/\Sigma|F_0|$ (based on reflections with $F_0^2>2\sigma F^2$). $wR_2=[\Sigma[w(F_0^2-F_c^2)^2]/\Sigma[w(F_0^2)^2]]^{1/2}$; $w=1/[\sigma^2(F_0^2)+(0.095P)^2]$; $P=[\max(F_0^2, 0)+2F_c^2]/3(F_0^2>2\sigma F^2)$.